Journal Pre-proof

Archaeological and environmental cave records in the Gobi-Altai Mountains, Mongolia

Nils Vanwezer, Sebastian F.M. Breitenbach, Fernando Gázquez, Julien Louys, Aleksandr Kononov, Dmitry Sokol'nikov, Avirmed Erdenedalai, Aitor Burguet-Coca, Andrea Picin, Arturo Cueva Temprana, Javier Sánchez-Martínez, William Taylor, Nicole Boivin, Bayarsaikhan Jamsranjav, Michael D. Petraglia

PII: S1040-6182(21)00136-1

DOI: https://doi.org/10.1016/j.quaint.2021.03.010

Reference: JQI 8802

To appear in: *Quaternary International*

Received Date: 9 November 2020

Revised Date: 3 March 2021

Accepted Date: 5 March 2021

Please cite this article as: Vanwezer, N., Breitenbach, S.F.M., Gázquez, F., Louys, J., Kononov, A., Sokol'nikov, D., Erdenedalai, A., Burguet-Coca, A., Picin, A., Cueva Temprana, A., Sánchez-Martínez, J., Taylor, W., Boivin, N., Jamsranjav, B., Petraglia, M.D., Archaeological and environmental cave records in the Gobi-Altai Mountains, Mongolia, *Quaternary International* (2021), doi: https://doi.org/10.1016/j.quaint.2021.03.010.

Archaeological and environmental cave records in the Gobi-Altai Mountains, Mongolia

Nils Vanwezer [a,*], Sebastian F.M. Breitenbach [b,*], Fernando Gázquez [c], Julien Louys [d], Aleksandr Kononov [e,f], Dmitry Sokol'nikov [g], Avirmed Erdenedalai [h], Aitor Burguet-Coca [i,j], Andrea Picin [a,k], Arturo Cueva Temprana [a], Javier Sánchez-Martínez [l], William Taylor [a,m], Nicole Boivin [a,n,o,p], Bayarsaikhan Jamsranjav [q], Michael D. Petraglia [a,n,o]

[a] Department of Archaeology, Max Planck Institute for the Science of Human History. Kahlaische Strasse 10, 07745 Jena, Germany
[b] Department of Geography and Environmental Sciences, Northumbria University. Newcastle upon Tyne, NE1 8ST, UK
[c] Water Resources and Environmental Geology, University of Almería, Carretera. Sacramento, 04120 Almería, Spain
[d] Australian Research Centre for Human Evolution, Environmental Futures Research Institute, Griffith University. Brisbane, Australia
[e] Institute of the Earth's Crust, Russian Academy of Sciences, Siberian Branch. Irkutsk 664033, Russia
[f] Irkutsk National Research Technical University. Irkutsk 664074, Russia
[g] Speleoclub Arabika. Irkutsk, Russia
[h] Mongolian Cave Research Association. Ulaanbaatar, 210523, Mongolia
[i] Institut Català de Paleoecologia Humana i Evolució Social (IPHES). Zona Educacional 4, Campus Sescelades URV (Edifici W3) 43007, Tarragona,Spain
[j] Universitat Rovira i Virgili (URV), Àrea de Prehistòria. Avinguda de Catalunya 35, 43002 Tarragona (Spain)
[k] Department of Human Evolution, Max Planck Institute for Evolutionary Anthropology. Deutscher Platz 6, 04103 Leipzig, Germany
[l] Centre d'estudis del Patrimoni Arqueològic. Barcelona, Spain
[m] Museum of Natural History, Henderson Building, University of Colorado-Boulder. Boulder, Colorado 80309, USA
[n] School of Social Sciences, University of Queensland. Brisbane, Queensland, Australia
[o] Department of Anthropology, National Museum of Natural History, Smithsonian Institution. Washington, D.C., USA
[p] Department of Anthropology and Archaeology, University of Calgary. Calgary, Canada
[q] National Museum of Mongolia. 210646 Ulaanbaatar, Mongolia

* Corresponding authors
E-mail addresses: vanwezer@shh.mpg.de (N. Vanwezer); sebastian.breitenbach@northumbria.ac.uk (S.F.M. Breitenbach)

Abstract

Though hundreds of caves are known across Mongolia, few have been subject to systematic, interdisciplinary archaeological surveys and excavations to understand Late Pleistocene and Holocene environments. Previous cave excavations in Mongolia have demonstrated their potential for preservation of archaeological and biological material, including Palaeolithic assemblages and Holocene archaeology, particularly burials, with associated organic finds. In other cases, cave surveys found that stratigraphic deposits and archaeological materials are absent. The large number of caves makes the Mongolian Altai Mountain Range a potentially attractive region for human occupation in the Pleistocene and Holocene. Here we present the results of an interdisciplinary survey of caves in four carbonate areas across the Gobi-Altai Mountains. We report 24 new caves, some of which contain archaeological material recovered through survey and test excavations. Most caves presented limited sedimentation, and some were likely too small for human habitation. Six caves showed evidence of palaeontological remains, mostly from likely late Holocene and recent periods. The most notable anthropogenic findings included petroglyphs at Gazar Agui 1 & 13. Gazar Agui 1 also contained lithics and a bronze fragment. Tsakhiryn Agui 1 contained 31 wooden fragments that include an unused fire drilling tool kit and items commonly found in association with medieval burials. We observed that the caves remain in contemporary use for religious and economic purposes, such as the construction of shrines, mining and animal corralling. Water samples from the caves, and nearby rivers, lakes, and springs were analysed for their isotopic compositions ($\delta^{18}O$, δD, $\delta^{17}O$, $^{17}O_{excess}$, d-excess) and the data, combined with backward trajectory modelling revealed that the Gobi-Altai region receives moisture mainly from western sources. These results form a baseline for future archaeological, paleoclimate and palaeoecological studies about regional seasonality and land use.

Keywords : Geomorphology; Speleology; Survey; Holocene; Archaeology; Water stable isotopes

1. Introduction

Caves across Central Asia demonstrated an extraordinary preservation potential for Pleistocene and Holocene deposits (Glantz et al., 2008; Bemmann and Nomguunsüren, 2012; Buzhilova et al., 2017). Caves provide stable microclimatic conditions and they are often more resistant to erosional processes compared to open-air contexts, making them an ideal scenario to investigate human activities (Straus, 1990), and climatological changes over time (Fairchild and Baker, 2012).

A series of key discoveries have been made in caves across Central Asia in recent years. Caves such as Obi Rakhmat and Teshik Tash, in Uzbekistan, contained skeletal elements demonstrating the presence of Neanderthals in eastern Eurasia. At Denisova Cave in the Russian Altai, hominin fossils have been recovered, allowing for proteomic analyses (including Zooarchaeology by Mass Spectrometry) (Brown et al., 2016) and ancient DNA studies (Krause et al., 2007; 2010; Meyer et al., 2012) including on sediments (Slon et al., 2017b). These studies led to the identification of the Denisovans in the Altai (Krause et al., 2010; Meyer et al., 2012; Slon et al., 2017a), as well as in the Qinghai Mountains in China (Chen et al., 2019; Zhang et al., 2020).

While there has been progress with recovering intact Palaeolithic sites in Mongolia, most recent investigations have been limited to open-air sites (Rybin et al., 2017; 2020; Khatsenovich et al., 2018; 2019; Zwyns et al., 2019; Marchenko et al., 2020), where organic preservation is unfortunately low (Zwyns et al., 2014). A notable exception for the recovery of hominin remains was a single, isolated skullcap at Salkhit, demonstrating the presence of *Homo sapiens* in Mongolia at 32 ka cal BP, with genetic information indicating Neanderthal and Denisovan ancestry (Devièse et al., 2019; Massilani et al., 2020). Tsagaan Agui, in the Gobi-Altai Mountains of Mongolia provides the earliest evidence of cave use, possibly dating as far back as ~520 ka BP and up until 32 ka BP (Derevianko et al., 2000a). Given the long history and density of stone tool assemblages at Tsagaan Agui, a repeated use of this cave over time is clearly indicated. The lithic assemblages from Tsagaan Agui illustrate that early and later Palaeolithic populations procured and made tools from a chert outcrop located above the cave (Brantingham et al., 2000; Derevianko et al., 2004). Faunal remains in the upper layers, dated to ~227ka BP (RTJI-804) – 33 ka BP (AA-23159) and <0.931 ka BP (AA-26586), contained large and small animals (Derevianko et al., 2000a), avian bones representative of 30 taxa, and ostrich eggshell (Martynovich, 2002). The identification of three hominin species (i.e., Denisovans, *H. neanderthalensis*, *H. sapiens*) in the greater region, including their mixed ancestries and overlapping occupations, has stimulated new explorations for caves in the rest of Central and Eastern Asia (Li et al., 2018; Cuthbertson et al., 2020; Iovita et al., 2020), raising interesting questions about the dispersal of *H. sapiens* across Asia (Li et al., 2019; Zwyns et al., 2019).

The earliest archaeological examples of cave use in the Holocene of Mongolia come from the rockshelter Chikhen Agui, located in the Gobi-Altai Mountains, where deposits date to ca. 11-7 ka BP (Derevianko et al., 2003; 2008). Despite the limited sedimentary record in the rockshelter, stone tools, ostrich egg beads, faunal remains, and 44 hearths were reported (Derevianko et al., 2003), implying that the shelter was used as a seasonal hunting station. Chikhen Agui contains a variety of raw material not available in the vicinity of the site and that can likely be linked to highly mobile seasonal groups. Other prehistoric examples of cave use are only known from rock art, which throughout Mongolia have been typologically dated from the Palaeolithic to the present (Terguunbayar and Ankhsanaa, 2019), with the majority dating from the Bronze Age to the Iron Age (Terguunbayar and Ankhsanaa, 2019). Currently, apart from rock art and Chikhen Agui, little is known about cave use during these later prehistoric periods.

The most frequent use of caves in Mongolia took place during the historic period, mainly for human burials (referred to as “cave and crevice burials”) approximately from the 5th century cal AD to the 19th century cal AD (Ahrens et al., 2015). Interments are frequently found in the southern arid regions of Mongolia and usually characterised by the burial of single individuals on the surface or in small rock crevices and caves (with cave entrances sometimes blocked off) (Erdenebat, 2009b; 2016; Bemmann and Nomguunsüren, 2012). Occasionally, interments include group burials or even murder victims, such as in Hets Mountain Cave (Frohlich et al., 2009). Such burials were first reported in the 1920s, and due to their remote locations, many of these sites have only recently been discovered (Erdenebat, 2009b). Cave burials often demonstrate complex and intricate burial practices, particularly in the choice of materials placed with the deceased. These burials frequently incorporate wooden caskets made out of pieces from carts (Ahrens et al., 2015), with wooden slats and/or threaded sticks as the base (Erdenebat and Chunag, 2015). Later, 15-17th century examples of burials show different wood structures such as ger lattices, like at Khuiten Khoshuu (Erdenebat and Bayar, 2004). While these practices are also common among open air stone covered graves, the excellent wood preservation in dry cave burials makes them unique

(Erdenebat, 2016). The organic preservation is often excellent, and recovered items include bows, quivers, arrows with feathers, musical instruments and saddles (Törbat et al., 2009; Nomguunsuren et al., 2012; Ahrens et al., 2015). Clothing such as *deels*, shoes and necklaces provide rare textile evidence of various time periods (Erdenebat and Bayar, 2004; Erdenebat, 2014; Pearson et al., 2019). Skeletal material frequently preserves skin, hair and bones of the deceased (Frohlich et al., 2009), and provides opportunities for radiocarbon dating, and isotope and aDNA analyses (Turner et al., 2012; Ahrens et al., 2015). The dry, stable, and largely abiotic environment in caves across Mongolia offer a wealth of information about burial practices in the past.

Central and southern Asian caves have been used extensively for religious purposes, particularly for practice of Buddhism, since historical times. The Tibetan form of Buddhism has been present in the Mongolian region for ~2000 years and has varied in popularity among the populace, but it first became politically significant in the 13^{th} century AD under Kublai Khan (Bira, 2009). Caves are important locations for Buddhists - Buddha spent much time meditating in caves, and they therefore represent the ascetic and hermetic values espoused by him (Barnes, 1995). Cave temples, such as those in nearby Magao, China, are frequently carved and mined out (Monteith, 2017). However, in Mongolian Buddhist practices, natural caves occur frequently as unmodified sections of monastery complexes (Charleux, 2003), or as individual sacred caves denoted by ceremonial blue scarves (*khadags*) (Lundberg et al., 2008). Buddhist activities in caves are recorded archaeologically in Mongolia, with evidence of ceramics and birchbark texts found in the upper layers of Tsagaan Agui (Derevianko et al., 2000a) and painted script on cave walls in Hurtsyin Agui

(Komatsu and Olsen, 2002). The total number of such examples in Mongolian caves remains uncollated as they are geographically dispersed (Olsen, 2003).

In addition to archaeological information, caves host some of the best terrestrial archives of past climatic and environmental conditions as their sedimentary deposits (unconsolidated sediments or speleothems) remain largely protected from harsh surface conditions (Fairchild and Baker, 2012). Speleothems (stalagmites, stalactites, flowstones) that form from infiltrating water under vadose conditions can be dated using U-series methods (Vaks et al., 2020). These create palaeoenvironmental archives that offer detailed chronologies covering millions of years as well as seasonal to centennial scale multi-proxy reconstructions of past climatic and environmental changes (Fairchild and Baker, 2012; Baldini et al., 2021).

While speleothems are widely used in many parts of the world for environmental reconstructions (Comas-Bru et al., 2020), there is a lack of speleothem-based reconstructions in Mongolia. Although earlier work by Vaks et al. (2013) showed that aridity limits speleothem deposition in parts of Mongolia, the wetter north-western regions (e.g., near Khovsgol lake) are likely more conducive for speleothem formation. Speleothem-based paleoclimate records routinely include stable oxygen and carbon isotope ratios, which inform on regional moisture history (e.g., source, amount, seasonal distribution) and local hydrological and ecological conditions (e.g., local aridity, soil and vegetation activity and composition). Combined with other geochemical proxies (e.g., trace metals) and environmental monitoring, detailed insights can be gained into past environmental changes and extreme events that place the archaeological data into a wider ecological context. Monitoring of environmental parameters, especially the isotopic composition of meteoric (precipitation, river, cave) waters, is of vital importance for correct interpretation of speleothem-based proxies (Lachniet, 2009; Breitenbach et al., 2015; Baldini et al., 2021).

Given the potential of recovering cultural and environmental information from caves in Mongolia, our team implemented an interdisciplinary archaeological survey and testing programme in the Gobi-Altai region. The main goals of the project were to locate caves and examine them for palaeoenvironmental information, as well as to identify archaeological deposits for reconstructing the human occupation history of the area. Here we report on visitation to 25 newly and formerly identified caves, with descriptions of their geographical contexts and archaeological finds. We also discuss the geomorphological history of the region, the taphonomic records of the caves, as well as the environmental proxies that have a bearing on preservation conditions.

2. Geographic background

The geographic range of the present interdisciplinary cave study encompassed two Mongolian *aimags* (provinces), Gobi-Altai (N 45.5°, E 95.5°) and Bayankhongor (N 46.1°, E 100.7°, Fig. 1). Major geographic features include the Khangai Mountains in the north, the Gobi-Altai Mountains that run West-East through the centre of the region, the Valley of the Gobi Lakes situated between both mountain ranges, and the Gobi Desert to the south, making the entire region a ‘basin and range’ physiography (Cunningham, 2013), with altitudes ranging between ca. 1100 and 3000 m above sea level (a.s.l.).

The modern climate of the region is broadly characterized as arid cold steppe (BSk) or desert (BWk) in the Köppen-Geiger classification (Peel et al., 2007). The region's hydrology varies from a sub-humid north, to a semi-arid centre, and an arid south (Endo et al., 2006). Precipitation is mainly derived from recycled moisture from westerly circulation from western Eurasia and the North Atlantic realm (Li et al., 2007; Burnik Šturm et al., 2017; Huang et al., 2017). Precipitation is highest in summer (Burnik Šturm et al., 2017), Fig. 2), mainly in the form of thunderstorms and hail storms (Lkhamjav et al., 2017). In recent decades the number of wet days and heavy rainfall events has significantly increased (Endo et al., 2006). Average modern temperatures range from ca. 20°C in July to -18°C in January (Fig. 2). During winter much of the region is covered by snow, which is mostly deposited on north- and leeward slopes. The region is largely unaffected by permafrost, except for isolated patches and sporadic permafrost in the Altai Mountains (Lehmkuhl et al., 2003; Zhao et al., 2010; Lehmkuhl, 2015). Micromorphological analysis of cryoturbated sediments (Bertran et al., 2003), vestigial cryoturbated features such as bedrocks and ice wedges (Owen et al., 1998), all suggest long periods of permafrost coverage throughout the region during glacials, but permafrost absence during interglacials.

2.1 Gobi-Altai Mountains

The Gobi-Altai Mountains comprise the south-eastern extension of the Altai Mountain Range (Fig. 1). The elevations in the region range from 1000-4000 m a.s.l., diminishing towards the southeast. The mountain ranges developed from the ongoing India-Eurasian continental convergence as part of the Cenozoic Central Asian orogenic system (Owen et al., 1999; Cunningham, 2013). The Gobi-Altai is primarily characterised by the many faults along the East-West facing Bogd fault system (Lamb and Badarch, 1997; Cunningham, 2013) that have constantly reworked the underlying geology since the Cretaceous (Balescu et al., 2007), with earthquakes as recent as 1957 (Ritz et al., 2003; Cunningham, 2013). These earthquakes have cut and disturbed the alluvial fan terraces (Ritz et al., 2003), and have also uplifted various plateaus and terrains around the Gobi-Altai to create the formations that characterise its modern appearance (Owen et al., 1997; van der Wal et al., 2020). The uplift of the Altai Mountains from the Miocene onward likely diminished the influx of moisture from the western sources, thereby intensifying aridification (Caves et al., 2014). Because of the faults, the underlying geology is a complex mix of different base lithologies (Cunningham, 2013): sandstone, porphyritic rhyolite, granite gneiss, quartz diorite, schist and others all exist in complex mélanges with each other (Kröner et al., 2007). The highly dynamic geological and climatic situation are not conducive to the formation and preservation of caves, and only about 20 cave localities had been reported in the Gobi-Altai region (Avirmed, 1999). This situation is aggravated by a significant sampling bias, due to the difficult access to this remote region.

Much of the vast terrain of the region does not contain karstifiable rocks and can be excluded as potential hosts of significant caves (Fig. 3). Old and frequently diagenetically overprinted sedimentary rocks, including limestones, marbles and carbonate-bearing arenites, are found along SE-NW oriented ranges (south of Jargalan) and more extensive patches in the centre (north of Altai) of the Zavkhan Terrane (Bold et al., 2016), as well as the western (near Bulgan) section of the study region. In this study, four areas (Tsakhiryn Nuruu, Aguin Nuruu, Saalit, and Gazar) were thoroughly explored for caves.

The high-altitude regions of the Gobi-Altai hosts some permafrost, whereas the lower altitude basins are permafrost-free. While the modern Gobi-Altai Mountains do not contain glaciers, there are some in the Khangai Mountains (northeast of the study region), as well as extensive glaciers in the main part of the Altai Mountains (Blomdin et al., 2016). The Khangai also contains palaeoglaciers, which had their largest extent during the local Last Glacial Maximum (LGM) ~40-35 ka BP (Rother et al., 2014). The Gobi-Altai is characterised by a stark lack of glacial features and it has been suggested that it only suffered intermittent glaciations (Ritz et al., 2003). Recent research, however, revealed that although asynchronous to the global trend of the LGM, glaciers formed in the region (Batbaatar et al., 2018). The same can be said for the Khangai Mountains (Rother et al., 2014). The presence of seasonal freshwater in mountain chains from melting glaciers and snow may have played an important role in facilitating early pastoralism (Taylor et al., 2020). The water flow from melting glaciers and snow patches and torrential rains supported the development of the large alluvial fans at the boundary between the mountains and the basins that characterise the present-day range (Owen et al., 1997). Most of these alluvial fans formed during the late Quaternary and coincide with large climatic shifts associated with glacial terminations, i.e., the transitions from cold/dry glacials to warmer and wetter interglacials (MIS 5 & 3 & 1) (Owen et al., 1997; Vassallo et al., 2005; 2011; Lehmkuhl et al., 2018; Malatesta et al., 2018; Klinge and Sauer, 2019). During the LGM, vegetation trapped aeolian sediments in the high altitudes of the Khangai and Gobi-Altai in concert with glacier formation, preventing the creation of new alluvial fans (Lehmkuhl et al., 2018; Malatesta et al., 2018). These aeolian sediments still cover most of the upper mountain but are currently being eroded and transported towards the basins.

2.2 Biogeography

Mongolia sits within the Palearctic province, and as such, it has zoogeographic affinities with both Europe and eastern Asia, a pattern that can be traced back to at least the early Neogene (Wang et al., 2013). The faunas that inhabit central Mongolia, and the Gobi-Altai in particular, have a limited faunal record relative to the wetter forested ecosystems in the north of the country. The reduced faunal record is largely limited due to local climatic, environmental, and geological conditions (Batsaikhan et al., 2010). The Mio-Pliocene fossil record of Mongolia is moderately well-understood although major Quaternary faunal units are absent so far (Wang et al., 2013). While the Middle Pleistocene Nalaikhan Formation in northern Mongolia has produced important microfaunal records (Erbajeva and Alexeeva, 2013), Quaternary fossils from the Gobi-Altai have only been described informally in the archaeological literature, with only extant species listed (Derevianko et al., 2000a; 2008).

Accumulation of skeletal remains in caves is often the result of biotic factors, with many vertebrate deposits in caves of allochthonous origin. Major biotic agents are cavernicolous species such as birds of prey or carnivorous mammals. Mongolia has a high diversity of diurnal birds of prey (Vaurie, 1964), including many that frequent caves and deposit pellets therein. Access to freshwater sources also play significant roles in the biogeography of arid environments, particularly in endorheic basins where most lakes are hyper-saline (Kaczensky et al., 2010; Payne et al., 2020).

Biogeography can strongly influence the likelihood of biotic accumulating agents (Louys et al., 2017). In the Gobi-Altai, several species of carnivores frequent or use caves, rock crevices, and burrows and might conceivably contribute to faunal records of caves. Canids, such as the foxes *Vulpes corsac* and *V. vulpes*, feed on small mammals, reptiles, and insects (Allen, 1938; Batsaikhan et al., 2010) and will often leave bones outside their dens (Batsaikhan et al., 2010). The Gobi bear (*Ursos arctos)* is also known to den in small caves, and its diet occasionally includes carrion (Allen, 1938; Batsaikhan et al., 2010). Small carnivores, such as *Felis silvestris, Otocolobus manul, Mustela eversmanni,* and *Martes foina* are also known to den amongst rocks (Allen, 1938; Batsaikhan et al., 2010). Finally, *Panthera uncia*, the snow leopard, hunts large prey (in addition to small mammals, birds, and insects) and frequently dens amongst rocks or in caves (Munkhtsog et al., 2016).

3. Materials and methods

3.1 Stable water isotopes

Stable isotopes of water are a useful tool for tracing processes related to the hydrological cycle, including moisture source history, convective dynamics, rainfall amount and secondary evaporation (Clark and Fritz, 1997; Lachniet, 2009). With recent analytical advancements, $\delta^{17}O$ and $^{17}O_{excess}$ of precipitation now complement the traditional $\delta^{18}O$, δD, and deuterium excess (d-excess) measurements. The advantage of measuring $^{17}O_{excess}$ is that it is less sensitive to temperature during evaporation than other isotopic parameters (e.g., d-excess) and is seemingly a robust tracer of relative humidity (RH) and precipitation formation processes (Luz and Barkan, 2010; Kaseke et al., 2017). In wet climate regimes, where re-evaporation of raindrops is minimal, $^{17}O_{excess}$ is linked to RH at the moisture source (i.e. the ocean surface) (Uechi and Uemura, 2019). In drier climates, $^{17}O_{excess}$ is likely overprinted by recycling effects, including re-evaporation of raindrops during rainfall if sub-cloud humidity is low (Landais et al., 2010; Tian et al., 2019). This is especially relevant for precipitation derived from continental moisture sources like in the case of Mongolia. Thus, using the triple isotope approach might help to identify and characterise the source and fate of moisture.

Although water stable isotopes are useful indicators of hydrological and atmospheric dynamics (Lachniet, 2009; Breitenbach et al., 2010; Kostrova et al., 2019) there is a dearth of data in Mongolia (Li et al., 2007; Yamanaka et al., 2007; Burnik Šturm et al., 2015; 2017). During the field trip, we collected a total of 22 water samples from rivers, springs, caves and precipitation for stable isotope analysis (SI Table 1). Additionally, we measured river and dripwater temperatures (SI Table 2). Samples of 5 to 12 mL were collected in plastic vials and analysed for oxygen and hydrogen ($\delta^{18}O$, $\delta^{17}O$, $^{17}O_{excess}$, δD, d-excess) isotopes using a cavity ring-down laser spectroscopy (CRDS) Picarro L-2140i, interfaced with an A0211 high-precision vaporizer (Picarro, Santa Clara, US) (Steig et al., 2014) at the University of Almeria, Spain. Each sample was injected ten times into the vaporizer, which was heated to 110°C. Memory effects from previous samples were avoided by rejecting the first three analyses. The results were normalized against Vienna Standard Mean Ocean Water (VSMOW) by analysing internal standards before and after each set of ten to twelve samples. To this end, three internal water standards were calibrated previously against VSMOW and SLAP, using $\delta^{17}O$ of 0.0‰ and -29.69865‰, respectively, and $\delta^{18}O$ of 0.0‰ and -55.5‰, respectively (Schoenemann et al., 2013). The $^{17}O_{excess}$ [$\ln(\delta^{18}O \div 1000 + 1) - 0.528 * \ln(\delta^{17}O \div 1000 + 1)$, (Barkan and

Luz, 2005)] and d-excess [δD – 8 * $\delta^{18}O$, (Dansgaard, 1964)] parameters denote deviations with respect to the global meteoric water line (GMWL). The $\delta^{18}O$, $\delta^{17}O$, $^{17}O_{excess}$, δD, d-excess are given in permil units (‰), while $^{17}O_{excess}$ is given in per meg (10^{-3} ‰). The ^{17}O-excess and d-excess were calculated for each injection using the corrected $\delta^{17}O$, $\delta^{18}O$ and δD values, and the last seven injections were used to calculate the mean values and analytical errors. The typical reproducibility (1 SD) of the analyses is better than 0.03 ‰ for $\delta^{17}O$, 0.04 ‰ for $\delta^{18}O$, 0.7 ‰ for δD, 0.4 ‰ for d-excess and 8 per meg for $^{17}O_{excess}$, based on repeated analysis of an internal standard (n=7) along with the samples during the run. Such high precision for the $^{17}O_{excess}$ determinations is due to the fact that isotope fractionations affecting oxygen isotopes during the analysis are mass-dependent; thus, the analytical errors for $\delta^{17}O$ and $\delta^{18}O$ covary and cancel out (Steig et al., 2014), keeping the $^{17}O_{excess}$ value virtually unaffected.

4. Results

4.1 Caves in the Tsakhiryn Nuruu (Limestone Mountains)

The Tsakhiryn Nuruu (Fig. 4) area is topped by the Ondoor-Tsakhir Mountain (2358 m) and drained by the Tsaagan Gol (Khuuray tsayran river in Soviet maps). The study region covers ca. 10 km^2, of which we surveyed the section west of the S-N running Tsaagan Gol. The peaks rise ca. 400 m above the river valley. Several ephemeral rivers and creeks drain the mountain. The region is accessed via the canyon that connects the villages of Khaliun and Tseel. Between these lies the eponymous rock art site of Tsaagan Gol (Kwang-jin et al., 2010b).

4.1.1 Tsakhiryn Agui 1

Tsakhiryn Agui 1 (Fig. 5) has a large, triangular-shaped entrance at the top of a massive debris cone. The cave formed in a carbonate breccia and it strikes SE-NW, sloping towards the NW. The main geomorphic features of this cave are the presence of massive breakdown blocks strewn over the entire length of the cave (ca. 36 m) and red calcite spar deposits near the entrance. The cave's orientation follows a major fracture through the host rock. Tsakhiryn Agui 1 does not feature vadose speleothems; the calcite spar is of phreatic origin.

We found thirty-one individual wood pieces (Fig. 6&7, Table 2) and one caprine horn on the surface and in the fractures between the boulders, scattered alongside bird bones, guano, and feathers. Two specific loci (Fig. 6D&E) contained most of the tool pieces and a smaller locus held a caprine horn and a single wood piece, all located in the upper right section of cave. There was hardly any sedimentation build up within the cave, except between the boulders. Two small fragments of wood were dated at the Oxford Radiocarbon Accelerator Unit (Table 3).

4.1.2 Tsakhiryn Agui 4

The Tsakhiryn Agui 4 (Fig. 8A) rockshelter is located near the top of the investigated mountain range (Fig. 8B). It consists of a southeast oriented and ca. 4-5 m deep main hall, with a smaller second deeper chamber, both with a floor of soft dusty sediment. The maximum depth of the cave is 7-8 m. The air temperature in the inner chamber was 12.8°C.

The excavation produced only natural clasts within a fine-grained unconsolidated sedimentary matrix derived from the host rock, of possible aeolian origin. We found no archaeological or faunal material. The bedrock of the rockshelter appeared at a maximum depth of 40 cm.

4.1.3 Irvesiin Agui

Irvesiin Agui (Snow Leopard Cave, named after a sighting, Fig. 9) is located in the southwestern slope of a small valley draining SE towards Tsaagan Gol. The cave's two main passages are oriented NW-SE, sloping towards the entrance and the valley. One of the passages has a total length of 39 m. The cave has a blocked passage at its NW extremity and a window at the very top. During the survey we also found evidence of occupation by *Panthera uncia* via excrement. The air temperature was 15°C in the southern and 13°C in the northern passage. The higher temperature in the southern passage is possibly due to better ventilation caused by the window atop the cave.

The cave's origin is likely phreatic, with subsequent remodelling during a vadose phase. Vadose conditions are evidenced by passage morphology, sediments, and remains of a flowstone found at the bifurcation of the two passages near the NE end. Two subsamples were collected from a ca. 13 cm thick flowstone sample (IA-18-1) for U/Th dating (performed at the Geochronology laboratory at the Johannes-Gutenberg University Mainz, Germany). Unfortunately, the sample is beyond the range of the U/Th method (i.e., >400 ka) and the age could not be determined. This sample consists of a layered translucent calcite with elongate crystal fabric, intercalated with numerous brownish/yellowish layers (Fig. 9C). Thin section microscopy reveals that the latter represent micritic particles that disrupt calcite growth, likely deposited in the wake of flood events that delivered suspended detritus in the cave passage.

Sub-millimetre size crystals (Fig. 9D) were found near the entrance and collected for X-ray diffraction analysis (Section 4.5). These crystals consisted of potassium nitrate (also known as saltpetre, which originates from the dung/guano in the cave) and traces of quartz. The passages show little sedimentation and the surfaces (including the flowstone) were covered by carnivore excrement and bone fragments.

4.1.4 Tsakhiryn Agui 1b, 2, 3, 5

Tsakhiryn Agui 1b is a small, ca. 5 m long cave north of Tsakhiryn Agui 1. The cave opens on the northern side of the debris cone that leads to Tsakhiryn Agui 1 and consists of a narrow passage strewn with rock debris and modern organic remains. Tsakhiryn Agui 2 is another 5 m long and NE-oriented cave with a small window to the northwest. The floor consists of rocks and sand, mixed with some animal excrements and modern microfauna. Tsakhiryn Agui 3, also a ca. 5 m long, is found in a SE-sloping layered limestone and seems to be the result of gravitational erosion processes rather than true karstification. We sampled dripwater at the far northern end. A large rockshelter, Tsakhiryn Agui 5, was found southwest of Tsakhiryn Agui 4 and at the same elevation. Like Tsakhiryn Agui 4, the cave is oriented SE, probably due to the geological orientation of the surrounding limestone. With a NW-SE extension of 14 m, the cave is larger than the others. The cave floor consists of rocks and sediments, however the window in the middle section of the cave, and a steep slope towards the exit suggest considerable and frequent sediment movement out of the cave. During the study, the mean cave air temperature was 17.2°C, the ground temperature was 13.5°C.

4.2 Caves of Aguin Nuruu

The Aguin Nuruu study area is located ca. 40 km west of the Tsakhiryn Nuruu region and part of the larger Khar Azargaiin Nuruu (Black Stallion Range) (Fig. 1). The 2200 m high mountain range drains towards the north through the Urd Uliastayn Gol (with its valley floor at ca. 1820 m altitude). The cave-bearing area is smaller than 4 km^2 and is largely restricted to carbonate pillars at the highest sections of these mountains; presenting therefore, limited potential for extended-use caves.

4.2.1 Nuramt Tsakhir Agui

Nuramt Tsakhir Agui (Powder Cave, Fig. 10) is located at 2092 m a.s.l. on the north side of the W-E oriented ridge just north of Zuslan Gol. The cave consists of a phreatically formed sub-horizontal passage with a total length of 11 m that slopes northwards. The cave ends in loose breakdown and the floor consists of dry soft sediment and larger host rock clasts. The air temperature inside the cave was 13.3°C. The cave has good ventilation due to the large entrance and open passage. There is evidence of recent use by a carnivore and/or birds of prey, as evidenced by the presence of a gnawed goat limb, feathers, and abundant scat.

The excavation produced no artefact finds, and bedrock was reached at a maximum depth of 70 cm. The excavated sediment consisted of a single layer composed of mechanically frost weathered angular limestone clasts in a fine aeolian silt matrix. We recovered several fresh micromammal and bird elements through sieving.

4.2.2 Khongil Tsakhir Agui

Khongil Tsakhir Agui (Mountain Tunnel Cave, Fig. 11) was found in a limestone cliff at 2025 m altitude. The cave is a ca. 63 m long complex maze and is easily visible from the Zuslan Gol valley. The cave system includes several eroded cave passages that belong to a single original cave system. The "main" entrance opens to the north, where a Tibetan Buddhist mantra, *Om mani padme om*, (Fig. 11C) is etched into the eastern wall. A small passage contained a votive miniature stupa (Fig. 11I). The main passage is a through-cave that exits the hosting butte, but there are also several side passages, including a longer tunnel towards the SE. The floor of the main passage consists of a shallow sandy and pebble-rich sediment layer, while the long SE-passage developed directly in the host rock. The entire system is a remnant of an older and much more extensive phreatic system. All the smaller side caves have sandy floors. The cave system contained a few bovid and horse skulls (Fig. 11D), and we found a fresh canid carcass in the southern part of the cave.

4.3 Caves in the Gazar region

The Gazar region is located north of the Altai Aimag centre and Taishir Soum (Fig. 2C). It forms part of the Zavkhan Formation in the larger Zavkhan Terrane (Bold et al., 2016) and presents a more open and complex morphology. The terrain is a hilly, treeless peneplain with altitudes between ca. 2000 m and 2500 m a.s.l., made of extensive basins and ranges with cliffs. Where carbonate outcrops are present, caves and grottoes are abundant. Water is only found in the river canyons (incised 30-100 m into the surface), a few intermittent creeks, the (now dammed) Zavkhan

Gol and seasonal Bayan Gol. Due to the difficult access, only a section of the ca. 150 km^2 large Gazar region was studied here.

4.3.1 Gazar Agui 1

Gazar Agui 1 is the only cave in the region with previously recorded coordinates, and it is located along a road that connects the Altai Aimag centre with Jargalan Soum. The cave is a horizontal passage with a wide, but relatively low entrance, currently used as a sheep pen and shelter (Fig. 12). The entrance to the cave is shielded by a wall made from cobbles of the cave arch exterior. The passage first follows a NW, then a NNE direction, with dimensions continuously diminishing as we move further away. Two cupolas at ca. 5 m and 13 m from the entrance allow standing space, but otherwise the ceiling is uniformly low. Gazar Agui 1 is characterized by the presence of thick dung and dust deposits. The goat dung is dried and used by herders as a seasonal combustible. We collected a single sample of the dripwater from the innermost passage. The cave air temperature was measured at 10.6°C.

Excavation of the cave (Fig. 12D&E), showed that the topmost 40 cm of sediment (Layer 1) consisted of modern sheep and goat dung intentionally left to dry, a common practice among nomadic pastoral Mongolia groups (Égüez and Makarewicz, 2018). Layer 1.1 was characterised by two darker and greyish soils and could be the result episodes of manure burning, similar to the Mediterranean sequences known as *fumiers* (Angelucci et al., 2009). Radiocarbon samples from the fumiers were dated as historic to recent (Table 4). The lowest level, Layer 2, is 1.4 m deep and composed of a dense matrix of cave spalls infilled with aeolian sediment. Faunal remains, including teeth, were found in all layers and consisted largely of micromammal and avian bones. We found a single flat corroded piece of bronze in the lower fumier of Layer 1.1.

The lithic assemblage was small and composed of lamellar artefacts (n=5) found in layer 1 and the upper part of layer 2 (Fig. 12C). The assemblage included two microblade fragments made on black chert, two microblade fragments made on grey chert and a single backed microblade fragment on grey chert.

4.3.2 Gazar Agui 2 & 3

A second noteworthy cave is Gazar Agui 2, which presents a large sediment cone below its entrance. The entrance is located 12 m above the valley floor and a few dozen meters east and below Gazar Agui 3. Inside we found micromammal bones, likely deposited by birds of prey, and modern refuse. The cave follows a NW and NE-ward trend, changing direction along major faults. It has a window above the main entrance. The total length of this cave is 54 m and shows significant traces of modern digging/mining. At about 10 m from the entrance, a ca. 2 m deep pit has been dug. At this first pit, we measured an air temperature of 10°C, while at the end of the cave it was 12.4°C. The sediment cone at the entrance was likely created by the mining carried out on the original sedimentary infill (sand/silt).

Gazar Agui 3, located a few meters above Gazar Agui 2, shares its origin with the latter. Both caves seem to have formed under phreatic conditions with calcite spar formation, and subsequent burial in unconsolidated sandy sediment under vadose conditions. The cave follows a northerly direction parallel to Gazar Agui 2 and consists of a single upward-trending passage. The floor is made up of sand and breakdown, from the collapse of the cave’s roof where a 10 m x 8 m chamber had developed. Beyond the collapsed area, the cave follows an increasingly narrow passage upwards to the surface. A human-made tunnel joins the natural passage from the west. At the exit of this abandoned mine, as well as in the deepest sections of the cave, we found calcite spar crystals up to 10 cm in length *in situ* and broken.

4.3.3 Gazar Agui 13

Gazar Agui 13 is a rockshelter located relatively close to the south of Gazar Agui 1. The rockshelter is formed on the side of an uplifted carbonate outcrop next to a small valley with a herding pen. The shelter is only 6 m x 5 m but contains large amount of soft sediment, which we excavated in a 1 x 1 m test pit (Fig. 13). The excavation yielded abundant microfaunal remains, including a relatively complete bird skeleton and fragmentary large mammal long bones. The taxa recovered included murids, pikas, and small birds. Bone preservation varied greatly, but showed no signs of burning. While some specimens appeared fresh, others exhibited staining which may be indicative of greater antiquity, suggesting mixing of the deposit. As in Gazar Agui 1, the upper layer of sediment consists of sheep and goat dung.

4.3.4 Gazar Agui 4-12

Several smaller caves (Gazar Agui 4 to 12) were explored and surveyed. The rock overlying the Gazar Agui 1 is riddled with smaller caves (including Gazar Agui 8, 11 and 12), indicating significant karstification. The orientation of these caves follows the limestone bedding and fault lines in NE-SW or NW-SE direction, which are consistent with that of the major tectonic features in the Gazar region. The caves Gazar Agui 4, 5, and 6 are remnants of phreatic tubes developed in the same hill as Gazar Agui 1 further south.

4.4 Caves in the Saalit region

Located in a low-lying outcrop amongst a steppe landscape (Fig. 2), Chikhen Agui is a previously excavated rockshelter. A brief survey was carried out around the surrounding hills of Chikhen Agui and the nearby spring. The survey yielded lithic artefacts ranging from the early Upper Palaeolithic to the Bronze Age, which is consistent with previously published information (Derevianko et al., 2003; 2008; 2015). The cherts vary between translucent patinated to opaque green or black types. Alongside nondiagnostic flakes and fragments, a blade fragment and a microblade, a side-scraper, a notched tool and two endscrapers were identified. It is worth noting a carinated bladelet core characterized by two lateral bladelet detachments on the carinated side and a flat platform created by a previous detachment. The opposed surface shows a bladelet production surface, and an attempt to rejuvenate the striking platform before discard. The other bladelet core is typical of the Neolithic/Bronze Age with a flaking surface exploited by pressure technique for the production of straight and regular bladelets and microblades. The core convexity was maintained through the thinning of the distal side and the preparation of a crest on the backside.

4.4.1 Saalit Agui 1

Saalit Agui cave is located in an adjoining outcrop, ~6 km away from Chikhen Agui. Embedded within a tilted lenticular limestone, the cave has been investigated for its ochre painted rock art (Derevianko et al., 1998; Vanwezer et al., 2020). Previous surveys reported a core and lithic blade fragments (Derevianko et al., 1998). In addition, the rock art displays several panels including anthropomorphs and “X” symbols produced from ochre, which possibly date to the Mesolithic. Re-examination of rock art at Saalit Cave took place during this fieldwork (Vanwezer et al., 2020), as did further survey of the canyons around it. Much of the surrounding region is composed of narrow winding ~3 m canyons and gullies, which most likely have seasonal streams.

4.4.2 Saalit Agui 2 & 3

Saalit Agui 2, like Saalit Agui 1, is located in a gully, created in the uplifted boundary between two intersecting uplifted geologies. It lies level with the bottom of the ravine and it has most likely been eroded by fluvial processes. The cave is small, ~2 m^3 and filled with modern-day detritus.

Saalit Agui 3 is a rockshelter located at the top of one of the ravines. It is clear that much of the roof and wall broke down, as there were many boulders and smaller rocks along the escarpment. This was possibly a result of the combination of fault movements and frost weathering. The inside is ~8 m wide, but only ~2 m deep, with no sediment accumulation, despite the large amount of sediment on the escarpment entrance.

4.5 Stable water isotopes

Water samples were collected from as many sites as possible in order to collate a baseline dataset against which results from future studies (e.g., on soil carbonates, speleothems or tooth enamel) could be compared to. This study provides not only $\delta^{18}O$ and δD, but for the first time also $\delta^{17}O$ values in this region. Rain, river, spring and dripwater $\delta^{18}O$ varies from -2.8 to -19‰, $\delta^{17}O$ from -1.5 to -10‰ and δD does from -18.1‰ to -143.6‰ (SI Table 1). The $^{17}O_{excess}$ varies from 7 to 61 per meg and the d-excess from -13.2 to 17.6‰. The mean $\delta^{18}O$, $\delta^{17}O$, δD, d-excess and $^{17}O_{excess}$ values (±1 SD) of the rain water samples (n=4) are -5.6±3.4‰, -2.9±1.8‰, -42.3±20‰, 2.4±11.8‰ and 20±11 per meg, respectively; for spring waters (n=12) are -11.8 ±3.8‰, -6.2±2.0‰, -88.0±29.1‰, 6.7±4.6‰ and 39±15 per meg, respectively; and for drip waters (n=6) are -7.1±1.9‰, -3.7±1.0‰, -56.1±7.8‰, 1.0±14.1‰ and 26±6 per meg, respectively.

The expression of the Local Meteoric Water Line (LMWL) for $\delta^{18}O$ vs δD is $\delta D = 6.9\ \delta^{18}O - 5.6$ (R^2=0.95, p<0.0001) (Fig. 14), and for $\delta^{17}O$ vs $\delta^{18}O$ is $\delta^{17}O = 0.53*\delta^{18}O + 0.025$ (R^2=1). The $^{17}O_{excess}$ is negatively correlated with $\delta^{18}O$ across the entire dataset (R^2=0.45, p<0.0006) (Fig. 15) and there is no significant correlation between $^{17}O_{excess}$ and d-excess (R^2=0.13) . When considering dripwater samples only, the negative correlation between $\delta^{18}O$ and d-excess is significant (R^2=0.75, p<0.03), while it is insignificant for $\delta^{18}O$ vs $^{17}O_{excess}$ (R^2=0.25, p<0.32). The river and dripwater temperatures vary from 5.6 to 21.2°C and 10.6 – 17.2°C, respectively. We find a tentative negative correlation (R^2=0.4, p=0.05) between river water temperature and altitude (995 to 2262 m a.s.l.). Such a link is not observed for dripwater, probably because the cave sites are located at very similar altitudes (2007 to 2092 m a.s.l.), giving a too narrow data spread. The correlations between water temperature and all the stable isotope parameters are insignificant , except for $^{17}O_{excess}$ in dripwater, which shows a positive correlation with water temperature (R^2=0.69, p=0.083). A larger database would be required to fully confirm such relationships.

5. Discussion

5.1 Environment and biogeography

5.1.1 Water Isotopes

The water samples we collected north of the Gobi Altai mountains (SI Fig. 1) during the 2018 survey fall very close to the GMWL and confirm the LMWL developed by Yamanaka et al. (2007) for northern Mongolia (Fig. 14, SI Fig. 1). This agreement helps reveal the processes that influence the isotopic signal of precipitation. Some of the rain- and dripwaters fall slightly below the GMWL, indicating significant re-evaporation during summertime rainfall events. Our results starkly contrast with data from the Gobi Desert, southwest of the Gobi-Altai Mountains (SI Fig. 1), published by Burnik Šturm et al. (2015, 2017). This dataset from the Gobi Desert has an intercept of -23.9‰, well below the GMWL (intercept = +10‰, Fig. 14), typical for precipitation in an arid region that is strongly affected by re- evaporation during and after rainfall (Burnik Šturm et al., 2017). Open waters (including lakes, marshes and puddles, well and spring samples) show lower d-excess and higher $\delta^{18}O$ values, suggesting that they are more affected by secondary evaporation, while rivers are somewhat less affected and closer to the regression line of the local precipitation.

The relatively high d-excess values (0 - +18 permil) in our dripwater, rainwater and river waters from the northern side of the Gobi-Altai suggest that most samples are derived from a source with high humidity (RH >70%) during evaporation (Clark and Fritz, 1997). A few rain- and dripwater samples show very low d-excess values and at the same time high $\delta^{18}O$ values, indicating secondary evaporation during/after precipitation (Bershaw, 2018). These samples are also located below the LMWL (Fig. 14). The effect of secondary evaporation on these samples is also evident in the observed negative relationship between $\delta^{18}O$ and $^{17}O_{excess}$ (Fig. 15). Although this trend is weak (R^2 = 0.45, p = 0.0006), all rain- and dripwater samples show high $\delta^{18}O$ and low $^{17}O_{excess}$ values. River waters, on the other hand, show lower $\delta^{18}O$ and higher $^{17}O_{excess}$ values, due to the integration of more winter derived runoff that is less affected by secondary evaporation. The observed difference in the isotopic composition of summer and winter precipitation can support future work on fossil waters (e.g., trapped in speleothem fluid inclusions).

We combine $\delta^{18}O$ and d-excess of rainwater (Fig. 16) to tentatively differentiate moisture sources and evaporation history for samples from Mongolia. We support our interpretation with backward trajectories assessments of individual precipitation samples using the Hybrid Single-Particle Lagrangian Integrated Trajectory (HYSPLIT) model (https://www.ready.noaa.gov/HYSPLIT.php, Stein et al., 2015). Backward trajectories were run for 96 hours from the day a sample was collected, with the start point being the sampling site. Trajectories originated at 1000, 2500 and 3500 m above ground. In Fig. 16 we discern two larger clusters , one with high d-excess values (> ca. -15‰) and one with d-excess values < ca. -15‰, but with similar $\delta^{18}O$ values. A third cluster comprises snow samples collected south of the Gobi Altai mountains by Burnik Sturm et al. (2017). The first two clusters are delineated by their geographic origin (SI Fig. 1) The upper cluster 1 comprises samples collected northeast of the Gobi-Altai Mountains, whereas the lower cluster 2 includes samples from the hyper-arid Gobi Desert southwest of the Gobi-Altai. These, and the snow samples of the left cluster 3 have been reported in Burnik

Sturm et al. (2017). The clusters are clearly separated even when only direct precipitation samples are considered, and surface waters are ignored.

HYPSLIT backward trajectories (not shown) reveal that nearly all these samples originated in the west. The upper cluster 1 includes precipitation sourced from the Westerlies during spring and summer, when relative humidity at the source is higher and d-excess is high, like in April and May 2003 (Fig. 16). The d-excess is then lowered during secondary re-evaporation. The lower cluster 2 is also Westerlies derived, but the distinctly lower d-excess values (<-4‰) point to different evaporative conditions at the moisture source. Earlier work in continental environments (e.g., Bershaw et al., 2016; Bershaw, 2018) linked extremely low d-excess values with recycling of water sourced from arid, highly evaporative closed-basin regions. Such recycling of continental surface waters from arid Central Asia, and secondary enrichment after precipitation in the Gobi Desert, would well explain the d-excess values found in cluster 2. HYSPLIT analysis reveals that cluster 2 samples tend to originate from continental westerly localities, but with higher variability of the source region. Finally, cluster 3 includes all samples with the most negative $\delta^{18}O$ values and d-excess values around -10‰. These are all snow samples and, according to HYSPLIT analysis, exclusively derived from the west.

Thus, the Gobi-Altai Mountain Range, reaching 3000 m a.s.l., acts as a geographic divide that separates these two hydrological systems.

5.1.2 Biotic seasonality

Our isotope dataset demonstrates that moisture for caves and rivers is mainly derived from westerly precipitation. These isotope results provide a baseline for the reconstruction of current and past diets of fauna and people (Sponheimer and Lee-Thorp, 1999). Precipitation and its seasonality also have important implications for the vegetation and insect availability of the mountainous steppe, which are the main sources of energy for the lowest trophic levels in the Gobi-Altai (Cheng et al., 2011; Zhu et al., 2014). Freshwater and grass are both severely impeded by winter freezing, precipitation and temperature changes (Munkhtsetseg et al., 2007), but it is clear that groundwater plays also important role in the region (Murdoch et al., 2017). Springs are a large continuous source of water, unlike the more seasonal and variable (especially summer) precipitation. Large fauna is heavily dependent on both of these water sources (Tumendemberel et al., 2015; Murdoch et al., 2017; Payne et al., 2020). However, when water freezes, ungulates such as argali (Murdoch et al., 2017), gazelle (Ito et al., 2013) and wild ass (Payne et al., 2020) migrate to areas with liquid water sources. The same generally occurs with nomads and their livestock, who migrate winter-spring/summer-autumn in search of pastures and shelter (Fijn, 2011). Modern herders still use spring water sources in winter by breaking the ice, providing water for wild animals (Murdoch et al., 2017).

Understanding past seasonality in humans and animals is difficult due to the lack of baseline records and the complexities of interpreting isotope data from fauna. Our initial water isotopes will help elucidate this, through comparison with archaeological observations of isotope values. In general, hunter-gatherers follow seasonal movements of large mammal migrations (ungulates in particular) which avoid dry, and frozen regions. Larger birds of prey such as eagles and raptors migrate south to the Himalayas and Korea during the winter (Vaurie, 1964; Batbayar et al., 2008; Batbayar and Lee, 2017). Rodents and lagomorphs burrow and hibernate during this period (Batsaikhan et al., 2010). Top level terrestrial carnivores such as snow leopards, bears and wolves do not migrate, as they are particularly suited to cold climates and den in caves (Batsaikhan et al., 2010; Munkhtsog et al., 2016). Former glaciers and ice patches may have played a role in increasing the access to freshwater at high altitude (Taylor et al., 2020). Our isotopic baseline may help establish future research on the role of extinct glaciers and ice patches as sources of water for humans and fauna. These seasonal variations in access to freshwater and food had most likely a significant impact on the spatial distribution of past human occupation of the mountainous regions of the Gobi-Altai.

5.2 Site and cave formation

Our surveys in the Gobi-Altai Mountains have shown three main contributors to the life history and use of caves. The first agents to consider are abiotic geomorphological processes that affect accumulation of sediments and minerals in cave environments. The second contributor includes fauna occupying the caves which may build up a moderate amount of debris. The third factor is human presence, which has been continuous in the region from the Late Pleistocene and up to the present.

5.2.1 Geomorphological and natural formation processes

Due to the extreme aridity of the Gobi-Altai, its karstic areas have developed much slower compared to many other regions in the world. We found evidence of extensive development of the caves below the water table; particularly in the Gazar region. In the Aguin and Tsakhriyn Nuruu regions, however, erosion at their higher altitudes has created a more dramatic landscape, in which the caves are presently at the top of remaining limestone outcrops. With a slightly lower altitude, the Tsakhiryn Nuruu region still demonstrates phreatic origins with the occurrence of calcite spar in Tsakhir Agui 1 and vadose conditions at Irvesiin Agui, where its flowstone indicates repeated periods of flooding. The age of the speleothem beyond the U/Th limit suggests that this region has been arid for a long time.

At Gazar, the majority of the caves were dry and level with or near the groundwater table and formed under semi-phreatic conditions. The calcite crystals at Gazar 2 and 3 attests to the presence of vadose conditions. Caves in the north are likely drier due to a colder, more periglacial environment (Komatsu and Olsen, 2002). Much of the water input is also seasonal, as during winter the freezing of the solutional cave walls provokes the spalling of large angular clasts, as evidenced in Layer 2 of Gazar Agui, and Nuramt Tsakhir Agui.

Sedimentation is low in many caves and this can be attributed to the orientation of their opening. Sediment in the caves may originate from the glacial aeolian sedimentation that occurred as a result of the drying of palaeolakes in the basins below the Gobi-Altai lakes. These cave sediments are likely related to the aeolian sediment covers found on the current mountain sides (Lehmkuhl et al., 2018), and all of the south and southeast facing caves show moderate to significant sediment deposition. Frost wedging likely produced the very common, smaller, angular clasts observed in most of the excavations we conducted. A rarer, but likely more modern cave deformation process is that of earthquakes and tremors that cause large boulder collapses from the cave walls. Much of the region is subjected to 4.5-5.5 magnitude earthquakes (recorded 1900-2000) with occasional strong ones such as the 8.1 magnitude in 1957 (Cunningham, 2013). These frequent seismic events likely contributed to the large amount of debris that we see in Tsakhiryn Agui 1, Saalit Agui 3, and Gazar Agui 13 (where two faults are visible in the cave). It seems that many of the geological and hydrological processes that created the caves in the Gobi-Altai Mountains are no longer active to the same degree, suggesting that these caves are relatively stable, barring catastrophic events such as earthquakes.

5.2.2 Biogenic accumulations

Most of the caves we explored, even those without sediment to excavate, presented some evidence of faunal activity. In Tsakhriyn Agui and Nuramt Tsakhir feathers and guano were scattered all over sediment and boulders. In the aforementioned caves, we did not recover large bone accumulations. In Gazar Agui 13 we found a large pellet with microfauna and recorded micromammal bones on the surface of many of the caves. This mirrors the large accumulation of samples from Dinesman's (1989) excavations. In the surveyed area of Irvesiin Agui, it was clear that extended *P. uncia* occupation lead to the accumulation of saltpetre deposits. In other excavated caves, such as Gazar Agui 1 and Nuramt Tsakhir Agui, avian and micromammal bones were commonly recovered from sieves, similarly to the sieving at Tsagaan Agui (Martynovich, 2002). These latter occurrences suggest that birds of prey created these accumulations. In addition to fauna, several of the excavated caves presented root systems, which suggest recent stabilisation of cave floors.

At Gazar Agui 1 we also found small carnivore bones. While the region records large carnivores denning in caves, our excavations showed no carnivore accumulations of ungulate bones or skeletal remains of large carnivores. Mongolia also lacks durophageous rodents, which are known to produce large bone deposits in Europe, Africa, and Southeast Asia (O'Regan et al., 2011; Louys et al., 2017). The lack of specialised bone accumulating species in Mongolia, combined with the unfavourable topographic conditions for significant sediment accumulation, most likely account for the limited preservation of large bones in the caves.

5.3 Human interactions with caves

Apart from Chikhen and Tsagaan Agui, it appears that the use of caves has in general been low. Our survey programme has demonstrated this point, recording varied cave contexts with different natural and cultural depositional histories.

5.3.1 Prehistoric

In these newly explored caves of the Gobi-Altai region, Middle and Late Pleistocene material could not be identified. Although archaic humans persisted in southern Siberia into MIS 6 (Douka et al., 2019), their presence in Mongolia is limited to the two archaeological cave sites of Tsagaan Agui (Derevianko et al., 2000a; 2000b) and Chikhen Agui (Derevianko et al., 2008). Our survey in the surrounding hills of Chikhen Agui confirmed that the cave site was attractive to human occupation over many periods, given the recovery of early Upper Palaeolithic to the Bronze Age lithics, consistent with earlier findings.

At Gazar Agui 1, fine chert was used for lithic manufacture, and entirely distinct from Tsagaan Agui and Chikhen Agui. The density of material at Gazar Agui 1 is very low, whereas the density of microblades and core surface sites and Chikhen Agui are extremely high. Microblade production was present in Chikhen Agui, representing a dominant method in the region from ca, 15-11 ka cal BP to the Bronze Age ca. 3 ka cal BP (Janz et al., 2017). Based on the occurrence of microliths and the rock art at Gazar Agui 1 (Vanwezer et al., 2020), human presence most likely correlates with the Neolithic. The low density in comparison to other lithic assemblages, and presence of only fragmented microblades suggests this was not a knapping location and that the material found could represent discarded fragments from a brief occupation.

Despite the lack of extensive prehistoric archaeological material in all of the caves, it is clear that Gazar Agui 1 & 13 were used by human groups, as evidenced by the presence of rock art (Vanwezer et al., 2020). The first signs of human occupation were in the Neolithic or Bronze Age, as the petroglyphs differ from younger ochre rock art sites (Vanwezer et al., 2020). We suggest that during the Neolithic to Bronze Age, cave use was short, and was targeted for the production of rock art. Gazar Agui 1 is the only documented cave in Mongolia containing both petroglyph rock art and Holocene archaeological materials.

On the basis of our survey, other cave sites show no signs of prehistoric occupations, despite the fact that their elevated contexts near reliable freshwater sources, could have made them suitable for occupation. However, their difficult access may have posed a problem for most humans. In contrast, Chikhen-, Tsagaan-, and Gazar 1-Agui are located on flat terrain with accessible entrances and better visibility. High mountain caves likely suit pastoralists whose herding activities bring them into those mountain valleys seasonally, whereas lowland caves provide easily visible and accessible shelter for both hunter-gatherers and pastoralists.

Thus, while the Gobi-Altai is known for two iconic Palaeolithic cave sites, many of the high-altitude caves in the region do not share the same archaeological density. suggesting that Palaeolithic populations targeted more accessible locations, repeatedly visiting them, without forays into sites in elevated topographic situations. During the Bronze Age or later, populations began to briefly access higher caves, producing rock art for symbolic purposes.

5.3.2 Historic

Of the caves surveyed, only Tsakhiryn Agui demonstrates evidence of historic use through the recovery of wooden artefacts. The function of the majority of the wood pieces is difficult to ascertain, as pieces are fractured and cracked to some degree and present no evidence of intentional modification. Those artefacts that do (Fig. 7), may be components of fire making kits (Jiang et al., 2018), particularly using the bow drilling technique. Other items are similar to those found in cave burials with wood remains. Dates on two of the wooden pieces suggest that the younger date (1117 ±40 cal AD, OxA-40026) is likely the closest to deposition date, placing the material in the medieval period. Or if the older date (251 ±13 cal AD, OxA-40028) indicates a separate earlier deposition, it could prove that there is reuse of Tsakhiryn Agui 1 over a 1000-year period.

Fire-making kits are not well known in Mongolian burials, and are largely limited to fire-strikers and flint (Erdenebat, 2009a). Despite a lack of comparable wooden fire-starting equipment from Mongolia, the Late Iron Age Yanghai cemeteries in China, present numerous examples of wood drilling tools with similar features (Jiang et al., 2018). That assemblage has hearths with similar prepared notches to help funnel embers. Jiang et al. (2018) claim that the Yanghai tools are for hand drilling and that recovered bows are more suitable for shooting. The bow fragment found at Tsakhiryn Agui appears to be designed for drilling, as burials of the period commonly have composite bows with arrows and quivers (Nomguunsuren et al., 2012; Ahrens et al., 2015). It is conceivable that any of the curved branches could be used as bows too, but most proper tools show working, such as the notches on the hearth and the nock on the bow. Despite this preparation, and unlike the tools at Yanghai, most of the pieces from Tsakhiryn Agui show no abrasion or charring. Particularly, none of the hearths show use either. Therefore, it is likely that these fire drilling tools form part of ceremonial assemblage or might have not had a chance to be used.

The other identifiable wooden items from Tsakhiryn Agui (Fig. 8) are more familiar components of recorded Mongolian burials. For example, the beam is a characteristic section of burials with cart parts (Miller, 2012; Ahrens et al., 2015), the ger lattice (Erdenebat and Bayar, 2004), and a whip handle [similar examples found at Tsagaan Khad and Ondor Khuren, see: Ahrens et al. (2015)] are common cave burial goods. Because looting is a common issue, the best preserved cave burials frequently present blocked off entrances to deny access to scavenging birds, carnivores, and looters (Ahrens et al., 2015). A nearby 15-16th century burial, Shandyn Amny Avst, lacks most of its skeletal elements (Kwang-jin et al., 2010a;

Bemmann and Nomguunsüren, 2012), likely because of the aforementioned reasons. We recovered no skeletal elements in Tsakhiryn Agui – so, if the wooden materials were once part of a burial, the burial would have been exposed. Despite possible destruction caused by exposure, the wood material at Tsakhiryn Agui reaffirms the impressive preservation environments of the caves in the Gobi-Altai.

The radiocarbon date of the wood to the medieval period, ceremonial nature of the wood drilling tools, and the wooden artefacts commonly associated with Mongolia cave burials suggest that the wood pieces found in Tsakhiryn Agui 1 are likely from a disturbed medieval cave burial site.

5.3.3 Recent

Of the 25 caves examined, five demonstrate signs of modern or recent historic usage. Buddhism returned to Mongolia in 1991 as one of the largest religious practices (Bira, 2009), possibly reclaiming previously used caves. Khongil Tsakhir Agui is clearly of importance to nearby herders. Their winter camp is located in the cave valley, near a stupa. The Buddhist mantra written on the outside of one of the entrances (Fig. 11C) is common throughout Mongolia, like in Alag Erdene in the north of Mongolia (Komatsu and Olsen, 2002). The bovid and equid skulls found on the cave floor (Fig. 11D), were likely placed as Buddhist offerings in concert with the miniature stupa (Fig. 11I). This practice is common throughout Mongolia, particularly with horse skulls, as a sign of respect to local spirits (Marchina et al., 2017). While Khongil Tsakhir Agui, shows no evidence of recurrent usage, Buddhist temple's Baishiya Karst Cave of the Tibetan Plateau (Chen et al., 2019) demonstrated the possibility of overlapping cave use, with its Denisovan skeletal remains. Under the right conditions, the same scenario could occur in the Mongolian caves. Due to the extensive historic presence of Buddhism in Mongolia, modern and archaeological Buddhist materials are widespread in caves.

Caprine faeces found in most of the caves surveyed indicate that they were used as shelters by the animals. Evidence from Gazar 1 & 13 differ from modern land use practices, as most recorded examples of corrals are open-air and made of wood, wire or stone (Égüez and Makarewicz, 2018). In many caves (e.g., Saalit 3, Tsakhiryn Agui 1) accumulations of goat droppings on the cave floors occur. In Gazar Agui 1 & 13, however, concerted penning efforts were present and large accumulations of dung were trampled and left to dry. Dried caprine dung is used today in much of arid Mongolia as a form of fuel where wood resources are lacking (Lkhagvadorj et al., 2013). These can be mass produced through corrals with caprines (Égüez and Makarewicz, 2018) or collected as individual pieces from larger animals (e.g. camels). At Gazar Agui 1 and 13, the use of this dung has likely removed and reworked the upper layer of the aeolian sediments (Layer 2), as well as earlier episodes of burning, thus the bronze piece and most of the lithic fragments found are in reworked contexts. The deliberate modification of Gazar Agui 1 through the creation of a wall from the cave spalls demonstrate an intentional investment towards reuse of the cave. Static structures such as caves and corrals are more likely to be revisited by seasonal nomads (Wright, 2016), and thus increase the chances of finding dense and reworked stratigraphic archaeological assemblages. Due to the extended history of pastoralist economic land use in Mongolia, it is likely that other caves throughout the country demonstrate a similar penning behaviour.

The radiocarbon dates of the fumier suggest that the dung drying behaviours at the cave are, at most, four centuries old. This method of penning occurs in other modern herding regions of the world (Égüez et al., 2018). However, numerous examples of penning and burning of dung also exist during the Neolithic to Iron Age of Europe (Angelucci et al., 2009; Burguet-Coca et al., 2020). In Central Asia there are a few past examples of cave corrals such as Chegirtke cave, Kyrgyzstan (Taylor et al., 2018), and Denisova cave in the Russian Altai Mountains was used as a sheep corral in the early Bronze Age (Derevianko and Molodin, 1994). While not widespread, it could be possible that this behaviour is more common in the mountainous regions of Mongolia and may have happened in the historic past.

Other modern anthropogenic interactions with caves include excavations and mining for calcite spars, as evidenced in Gazar Agui 2 & 3. Informal 'ninja' mining is currently a frequent occurrence across Mongolia, and the result of widespread environmental problems, leading to heavy livestock losses and consequent poverty (Grayson et al., 2004). These small-scale operations, which have increasingly become privatised (Munkherdene and Sneath, 2018), have a common goal of finding precious ores, particularly gold, but other minerals are also being targeted. Organised 'legal' mining efforts led to the discovery of the only Pleistocene fossil, the Salkhit skull. Despite this, they failed to recover any other contextual information (Günchinsüren, 2007), and as such, little was known about the sample until recent bioarchaeological analyses (Devièse et al., 2019; Massilani et al., 2020). The large-scale disturbances caused by these mining processes are clear in open landscapes, but the effects on cave systems are less visible. At Gazar Agui 2 & 3, we observed extraction of sediments and the removal of calcite spars, which resulted in the disruption of possible palaeoenvironmental, palaeontological or archaeological information. Although mining can be the source of archaeological discoveries, it can also negatively impact karstic environments and the cultural heritage associated with them.

6. Conclusions

Due to dramatic changes to the landscape in the Late Pleistocene and Early Holocene, there are still many unknowns regarding prehistoric land use practises. Although earlier surveys in northern and central Asia led to the discovery of caves with long stratigraphies containing archaeological materials, since then it has been difficult to identify additional caves with similar records. The dispersal of hominins throughout the Late Pleistocene in Northern Asia is still completely unknown. These targeted surveys provide contextual information for further exploration. Our survey team located, documented, and examined 25 caves from four regions in the Gobi-Altai Mountains in western Mongolia. We found that most caves do not contain Pleistocene records, which could suggest that hunter-gatherers preferred caves in low-lying steppe regions. The presence of Holocene archaeology suggests that pastoral seasonal behaviours were more suited to use mountainous caves. Cave burials and rock art represent the most common cave use in the study area. While indications of early hominin use are rare unlike the nearby Russian Altai, the landscape use of Holocene humans is evident at several caves. They provide a better understanding of the changing utility that caves provide over time in nomadic regions as cultural and economic locations. They also demonstrate the shared similarities in practices with nearby regions such as the Himalayas and Northern

Asia, exemplifying the expanded interconnectivity and population density that occurs towards the Late Holocene.

Environmental data is present in many caves, and the isotopic data from precipitation, surface water and drip water contexts provide a baseline for contemporaneous water sources, atmospheric dynamics, and for future biotic and speleothem analyses. This will be fundamental to understand the importance of mountain water sources for past people. Climate research is frequently detached from the humans that form an intrinsic part of it (Beckage et al., 2020), thus, this interdisciplinary work marks our attempt to integrate these two lines of research.

As a result of our extensive cave survey, we can conclude that south and south-east oriented cave entrances are more likely to contain sediment layers thick enough to preserve fauna and archaeological materials that provide information about environmental and behavioural dynamics. The recovered wooden medieval tools are prime examples of biological preservation in this climate. The aridity and extreme seasonality of the Gobi-Altai region means that today, and likely in the past, people had to migrate during colder periods. Given the large number of undocumented caves in the Gobi-Altai Mountains, we suggest that further concerted exploration is worthwhile, especially for the Palaeolithic, in contexts at the interface of low-lying areas with palaeolakes, palaeorivers, and springs.

7. Acknowledgements

Fieldwork and excavations conducted with the permission of the Ministry of Education, Culture, and Science for Mongolia. This research was funded by the Max Planck Society. AK was supported by the Ministry of Science and Higher Education of the Russian Federation (grant No. 075-15-2020-787 for implementation of "Fundamentals, methods and technologies for digital monitoring and forecasting of the environmental situation on the Baikal natural territory"). FG was financially supported by the “HIPATIA” research program of the University of Almeria. We thank everyone involved with fieldwork, Denis Scholz for the U/Th dating attempt, and Bryan Miller for access to key literature.

8. References

Ahrens, B., Nomguunsüren, G., Piezonka, H., 2015. Das mittelalterliche Höhlengrab von Cagaan Chad, Mongolei: Eine Kriegerbestattung am nördlichen Rand der Wüste Gobi. Zeitschrift für Archäologie des Mittelalters 43, 59–126.

Allen, G.M., 1938. The Mammals of China and Mongolia, Part 2. Natural History of Central Asia, vol. XI. American Museum of Natural History, New York.

Angelucci, D.E., Boschian, G., Fontanals, M., Pedrotti, A., Vergès, J.M., 2009. Shepherds and karst: the use of caves and rock-shelters in the Mediterranean region during the Neolithic. World Archaeology 41, 191–214. doi:10.1080/00438240902843659

Avirmed, E., 1999. The Caves of Mongolia (In Mongolian, Russian/English abstracts). Academy of Sciences of Mongolian Republic, Ulaanbaatar.

Baldini, J.U.L., Lechleitner, F., Breitenbach, S.F.M., Hunen, J. van, Baldini, L.M., Wynn, P.M., Jamieson, R.A., Ridley, H.E., Baker, A.J., Walczak, I.W.F.J., 2021. Detecting and quantifying palaeoseasonality in stalagmites using geochemical and modelling approaches. Quaternary Science Reviews. doi:10.1016/j.quascirev.2020.106784

Balescu, S., Ritz, J.-F., Lamothe, M., Auclair, M., Todbileg, M., 2007. Luminescence dating of a gigantic palaeolandslide in the Gobi-Altay mountains, Mongolia. Quaternary Geochronology 2, 290–295. doi:10.1016/j.quageo.2006.05.026

Barkan, E., Luz, B., 2005. High precision measurements of 17O/16O and 18O/16O ratios in H2O. Rapid Communications in Mass Spectrometry 19, 3737–3742. doi:10.1002/rcm.2250

Barnes, G.L., 1995. An introduction to Buddhist archaeology. World Archaeology 27, 165–182. doi:10.1080/00438243.1995.9980301

Batbaatar, J., Gillespie, A.R., Fink, D., Matmon, A., Fujioka, T., 2018. Asynchronous glaciations in arid continental climate. Quaternary Science Reviews 182, 1–19. doi:10.1016/j.quascirev.2017.12.001

Batbayar, N., Lee, H., 2017. Steppe Eagle Migration from Mongolia to India. In: Prins, H.H.T., Namgail, T. (Eds.), Bird Migration Across the Himalayas: Wetland Functioning amidst Mountains and Glaciers. Cambridge University Press, Cambridge, pp. 117–127.

Batbayar, N., Reading, R., Kenny, D., Natsagdorj, T., Kee, P.W., 2008. Migration and Movement Patterns of Cinereous Vultures in Mongolia. Falco 32, 5–7.

Batsaikhan, N., Samiya, R., Shar, S., Lkhagvasuren, D., King, S.R.B., 2010. A field guide to the mammals of Mongolia, 2nd ed. Zoological Society of London, London.

Beckage, B., Lacasse, K., Winter, J.M., Gross, L.J., Fefferman, N., Hoffman, F.M., Metcalf, S.S., Franck, T., Carr, E., Zia, A., Kinzig, A., 2020. The Earth has humans, so why don’t our climate models? Climatic Change 163, 181–188. doi:10.1007/s10584-020-02897-x

Bemmann, J., Nomguunsüren, G., 2012. Bestattungen in Felsspalten und Hohlräumen mongolischer Hochgebirge. In: Bemmann, J. (Ed.), Steppenkrieger:

Reiternomaden Des 7. – 14. Jahrhunderts Aus Der Mongolei. LVR-LandesMuseum Bonn, Darmstadt, pp. 199–217.

Bershaw, J., 2018. Controls on Deuterium Excess across Asia. Geosciences 8, 257. doi:10.3390/geosciences8070257

Bershaw, J., Saylor, J.E., Garzione, C.N., Leier, A., Sundell, K.E., 2016. Stable isotope variations (δ18O and δD) in modern waters across the Andean Plateau. Geochimica et Cosmochimica Acta 194, 310–324. doi:10.1016/j.gca.2016.08.011

Bertran, P., Fontugne, M., Jaubert, J., 2003. Permafrost aggradation followed by brutal degradation during the upper pleniglacial in Mongolia: the probable response to the H2 Heinrich event at 21 kyr BP. Permafrost and Periglacial Processes 14, 1–9. doi:10.1002/ppp.435

Bira, S., 2009. Buddhism in Mongolia. In: Fitzhugh, W.W., Rossabi, M., Honeychurch, W. (Eds.), Genghis Khan and the Mongol Empire. University of Washington Press, Seattle, pp. 272–274.

Blomdin, R., Heyman, J., Stroeven, A.P., Hättestrand, C., Harbor, J.M., Gribenski, N., Jansson, K.N., Petrakov, D.A., Ivanov, M.N., Alexander, O., Rudoy, A.N., Walther, M., 2016. Glacial geomorphology of the Altai and Western Sayan Mountains, Central Asia. Journal of Maps 12, 123–136. doi:10.1080/17445647.2014.992177

Bold, U., Smith, E.F., Rooney, A.D., Bowring, S.A., Buchwaldt, R., Dudas, F.., Ramezani, J., Crowley, J.L., Schrag, D.P., Macdonald, F.A., 2016. Neoproterozoic stratigraphy of the Zavkhan terrane of Mongolia: The backbone for Cryogenian and early Ediacaran chemostratigraphic records. American Journal of Science 316, 1–63. doi:10.2475/01.2016.01

Brantingham, P.J., Olsen, J.W., Rech, J.A., Krivoshapkin, A.I., 2000. Raw Material Quality and Prepared Core Technologies in Northeast Asia. Journal of Archaeological Science 27, 255–271. doi:10.1006/jasc.1999.0456

Breitenbach, S.F.M., Adkins, J.F., Meyer, H., Marwan, N., Kumar, K.K., Haug, G.H., 2010. Strong influence of water vapor source dynamics on stable isotopes in precipitation observed in Southern Meghalaya, NE India. Earth and Planetary Science Letters 292, 212–220. doi:10.1016/j.epsl.2010.01.038

Breitenbach, S.F.M., Lechleitner, F.A., Meyer, H., Diengdoh, G., Mattey, D., Marwan, N., 2015. Cave ventilation and rainfall signals in dripwater in a monsoonal setting – a monitoring study from NE India. Chemical Geology 402, 111–124. doi:10.1016/j.chemgeo.2015.03.011

Brown, S., Higham, T., Slon, V., Pääbo, S., Meyer, M., Douka, K., Brock, F., Comeskey, D., Procopio, N., Shunkov, M. V., Derevianko, A.P., Buckley, M., 2016. Identification of a new hominin bone from Denisova Cave, Siberia using collagen fingerprinting and mitochondrial DNA analysis. Scientific Reports 6, 23559. doi:10.1038/srep23559

Burguet-Coca, A., Polo-Díaz, A., Martínez-Moreno, J., Benito-Calvo, A., Allué, E., Mora, R., Cabanes, D., 2020. Pen management and livestock activities based on phytoliths, dung spherulites, and minerals from Cova Gran de Santa Linya (Southeastern pre-Pyrenees). Archaeological and Anthropological Sciences 12. doi:10.1007/s12520-020-01101-6

Burnik Šturm, M., Pukazhenthi, B., Reed, D., Ganbaatar, O., Sušnik, S., Haymerle, A., Voigt, C.C., Kaczensky, P., 2015. A protocol to correct for intra- and interspecific variation in tail hair growth to align isotope signatures of segmentally cut tail hair to a common time line. Rapid Communications in Mass

Spectrometry 29, 1047–1054. doi:10.1002/rcm.7196

Burnik Šturm, M., Ganbaatar, O., Voigt, C.C., Kaczensky, P., 2017. First field-based observations of δ 2 H and δ 18 O values of event-based precipitation, rivers and other water bodies in the Dzungarian Gobi, SW Mongolia. Isotopes in Environmental and Health Studies 53, 157–171. doi:10.1080/10256016.2016.1231184

Buzhilova, A., Derevianko, A., Shunkov, M., 2017. The Northern Dispersal Route: Bioarchaeological Data from the Late Pleistocene of Altai, Siberia. Current Anthropology 58, S000–S000. doi:10.1086/694232

Caves, J.K., Sjostrom, D.J., Mix, H.T., Winnick, M.J., Chamberlain, C.P., 2014. Aridification of Central Asia and uplift of the Altai and Hangay Mountains, Mongolia: Stable isotope evidence. American Journal of Science 314, 1171–1201. doi:10.2475/08.2014.01

Charleux, I., 2003. Buddhist Monasteries in Southern Mongolia. In: Pichard, P., Lagirarde, F. (Eds.), The Buddhist Monastery: A Cross-Cultural Survey. École Française d'Extrême-Orient, Paris, pp. 351–390.

Chen, F., Welker, F., Shen, C.-C., Bailey, S.E., Bergmann, I., Davis, S., Xia, H., Wang, H., Fischer, R., Freidline, S.E., Yu, T.-L., Skinner, M.M., Stelzer, S., Dong, G., Fu, Q., Dong, G., Wang, J., Zhang, D., Hublin, J.-J., 2019. A late Middle Pleistocene Denisovan mandible from the Tibetan Plateau. Nature 569, 409–412. doi:10.1038/s41586-019-1139-x

Cheng, Y., Tsubo, M., Ito, T.Y., Nishihara, E., Shinoda, M., 2011. Impact of rainfall variability and grazing pressure on plant diversity in Mongolian grasslands. Journal of Arid Environments 75, 471–476. doi:10.1016/j.jaridenv.2010.12.019

Clark, I.D., Fritz, P., 1997. Environmental isotopes in hydrogeology. CRC Press, Boca Raton.

Comas-Bru, L., Rehfeld, K., Roesch, C., Amirnezhad-Mozhdehi, S., Harrison, S.P., Atsawawaranunt, K., Ahmad, S.M., Ait Brahim, Y., Baker, A., Bosomworth, M., Breitenbach, S.F.M., Burstyn, Y., Columbu, A., Deininger, M., Demény, A., Dixon, B., Fohlmeister, J., Hatvani, I.G., Hu, J., Kaushal, N., Kern, Z., Labuhn, I., Lechleitner, F.A., Lorrey, A., Martrat, B., Novello, V.F., Oster, J., Pérez-Mejías, C., Scholz, D., Scroxton, N., Sinha, N., Ward, B.M., Warken, S., Zhang, H., the SISAL members, 2020. SISALv2: A comprehensive speleothem isotope database with multiple age-depth models. Earth System Science Data Discussions in review.

Cunningham, D., 2013. Mountain building processes in intracontinental oblique deformation belts: Lessons from the Gobi Corridor, Central Asia. Journal of Structural Geology 46, 255–282. doi:10.1016/j.jsg.2012.08.010

Cuthbertson, P., Ullmann, T., Büdel, C., Varis, A., Namen, A., Seltmann, R., Reed, D., Taimagambetov, Z., Iovita, R., 2020. Finding karstic caves and rockshelters in the Inner Asian mountain corridor using predictive modelling and field survey. EarthArXiv Preprints. doi:10.31223/osf.io/vz3b5

Dansgaard, W., 1964. Stable isotopes in precipitation. Tellus 16, 436–468. doi:10.3402/tellusa.v16i4.8993

Derevianko, A.P., Molodin, V.I., 1994. Denisova peshera I (in Russian). Nauka, Novosibirsk.

Derevianko, A.P., Olsen, J.W., Tseveendorj, T., Petrin, V.T., Zenin, A.N., Krivoshapkin, A.I., Reeves, R.W., Mylnikov, V.P., Nikolaev, S. V., Gunchinsuren, D., B., Yadmaa, T., Brantingham, P.J., Rech, J.A., 1998. Archaeological studies carried out by the Joint Russian-Mongolian-American Expedition in Mongolia in

1996. Novosibirsk.

Derevianko, A.P., Olsen, J.W., Tseveendorzh, D., Krivoshapkin, A.I., Petrin, V.T., Brantingham, P.J., 2000a. The Stratified cave site of Tsagaan Agui in the Gobi Altai (Mongolia). Archaeology, Ethnology and Anthropology of Eurasia 1, 23–36.

Derevianko, A.P., Devyatking, E.V., Simakova, A.N., Olsen, J.W., Kulikov, O.A., Gnibedenko, Z.N., 2000b. The Tsagan-Agui Cave (Mongolia): Pliestocene Stratigraphy, Archeology, and Paleoecology. Stratigraphy and Geological Correlation 8, 90–105.

Derevianko, A.P., Gladyshev, S.A., Nohrina, T.I., Olsen, J.., 2003. The Mongolian Early Holocene excavations at Chikhen Agui rockshelter in the Gobi Altai. The Review of Archaeology 24, 50–56.

Derevianko, A.P., Brantingham, P.J., Olsen, J.W., Tseveendorj, D., 2004. Initial upper Paleolithic blade industries from the north-central Gobi Desert, Mongolia. In: Brantingham, P.J., Kuhn, S.L., Kerry, K.W. (Eds.), The Early Upper Paleolithic beyond Western Europe. University of California Press, Berkeley, pp. 207–222. doi:10.1525/9780520930094-016

Derevianko, A.P., Olsen, J.W., Tseveendorzh, D., Gladyshev, S.A., Nokhrina, T.I., Tabarev, A. V., 2008. New Insights Into the Archaeological Record At Chikhen Agui Rockshelter (Mongolia). Archaeology, Ethnology and Anthropology of Eurasia 34, 2–12. doi:10.1016/j.aeae.2008.07.001

Derevianko, A.P., Markin, S.V., Gladyshev, S.A., Olsen, J.W., 2015. The Early Upper Paleolithic of the Gobi Altai region in Mongolia (Based on Materials from the Chikhen-2 Site). Archaeology, Ethnology and Anthropology of Eurasia 43, 17–41. doi:10.1016/j.aeae.2015.11.004

Deviése, T., Massilani, D., Yi, S., Comeskey, D., Nagel, S., Nickel, B., Ribechini, E., Lee, J., Tseveendorj, D., Gunchinsuren, B., Meyer, M., Pääbo, S., Higham, T., 2019. Compound-specific radiocarbon dating and mitochondrial DNA analysis of the Pleistocene hominin from Salkhit Mongolia. Nature Communications 10, 274. doi:10.1038/s41467-018-08018-8

Dinesman, L.G., Kiseleva, N.K., Knyazev, A.V., 1989. History of the steppe ecosystems of the Mongolian People's Republic (in Russian). Nauka, Moscow.

Douka, K., Slon, V., Jacobs, Z., Ramsey, C.B., Shunkov, M. V., Derevianko, A.P., Mafessoni, F., Kozlikin, M.B., Li, B., Grün, R., Comeskey, D., Devièse, T., Brown, S., Viola, B., Kinsley, L., Buckley, M., Meyer, M., Roberts, R.G., Pääbo, S., Kelso, J., Higham, T., 2019. Age estimates for hominin fossils and the onset of the Upper Palaeolithic at Denisova Cave. Nature 565, 640–644. doi:10.1038/s41586-018-0870-z

Égüez, N., Makarewicz, C.A., 2018. Carbon Isotope Ratios of Plant n -Alkanes and Microstratigraphy Analyses of Dung Accumulations in a Pastoral Nomadic Winter Campsite (Eastern Mongolia). Ethnoarchaeology 10, 141–158. doi:10.1080/19442890.2018.1510614

Égüez, N., Zerboni, A., Biagetti, S., 2018. Microstratigraphic analysis on a modern central Saharan pastoral campsite. Ovicaprine pellets and stabling floors as ethnographic and archaeological referential data. Quaternary International 483, 180–193. doi:10.1016/j.quaint.2017.12.016

Endo, N., Kadota, T., Matsumoto, J., Ailikun, B., Yasunari, T., 2006. Climatology and Trends in Summer Precipitation Characteristics in Mongolia for the Period 1960-98. Journal of the Meteorological Society of Japan 84, 543–551. doi:10.2151/jmsj.84.543

Erbajeva, M., Alexeeva, N., 2013. Late Cenozoic mammal faunas of the Baikalian region: composition, biochronology, dispersal and correlation with Central Asia. In: Wang, X., Flynn, L.J., Fortelius, M. (Eds.), Fossil Mammals of Asia: Neogene Biostratigraphy and Chronology. Columbia University Press, New York, pp. 495–507.

Erdenebat, U., 2009a. Altmongolisches Grabbrauchtum: Archäologisch-historische Untersuchungen zu den mongolischen Grabfunden des 11. bis 17. Jahrhunderts in der Mongolei. Rheinische Friedrich-Wilhelms-Universität Bonn.

Erdenebat, U., 2009b. Cave Burials of Mongolia. In: Fitzhugh, W.W., Rossabi, M., Honeychurch, W. (Eds.), Genghis Khan and the Mongol Empire. University of Washington Press, Seattle, pp. 259–261.

Erdenebat, U., 2014. Some findings of cave burial of Dund Nuruu, Bayan-Undur Soum, Bayankhongor Province [In Mongolian]. Studia Archaeologica Instituti Archaeologici Academiae Scientiarum Mongolicae 34, 344–365.

Erdenebat, U., 2016. Tombs and graves of the Mongolian era. In: Eregzen, G. (Ed.), Archaeological Relics of Mongolia III: Ancient Funeral Monuments of Mongolia. Ulaanbaatar, pp. 240–269.

Erdenebat, U., Bayar, D., 2004. Eine Mittelalterliche Felshöhlenbestattung aus der südlichen Mongolei. In: Beiträge Zur Allgemeinen Und Vergleichenden Archäologie. Verlag Philipp Von Zabern, Mainz.

Erdenebat, U., Chunag, A., 2015. Cave burial of Shiluudtei [In Mongolian]. Nomadic Heritage Studies 16, 123–135.

Fairchild, I.J., Baker, A., 2012. Speleothem Science: From Process to Past Environments. John Wiley & Sons, Ltd, Chichester. doi:10.1002/9781444361094

Fijn, N., 2011. Living with herds: human-animal coexistence in Mongolia. Cambridge

University Press, New York.

Frohlich, B., Tsend, A., Hunt, D.R., Hinton, J., Erdene, B., 2009. Forensics in the Gobi: The mummies of the Hets Mountain Cave. In: Fitzhugh, W.W., Rossabi, M., Honeychurch, W. (Eds.), Genghis Khan and the Mongol Empire. University of Washington Press, Seattle, pp. 255–258.

Glantz, M.M., Viola, B., Wrinn, P., Chikisheva, T., Derevianko, A.P., Krivoshapkin, A.I., Islamov, U., Suleimanov, R., Ritzman, T., 2008. New hominin remains from Uzbekistan. Journal of Human Evolution 55, 223–237. doi:10.1016/j.jhevol.2007.12.007

Grayson, R., Delgertsoo, T., Murray, W., Tumenbayar, B., Batbayar, M., Urtnasan, T., Dashzeveg, B., Chimed, E.-B., 2004. The People's Gold Rush in Mongolia – the Rise of the 'Ninja' Phenomenon. World Placer Journal 4, 1–112.

Günchinsüren, B., 2007. Introduction into Stone Age of Mongolia. In: Bemmann, J., Parzinger, H., Pohl, E., Tseveendorzh, D. (Eds.), Current Archaeological Research in Mongolia. Papers from the First International Conference on "Archaeological Research in Mongolia" Held in Ulaanbaatar, August 19th–23rd, 2007. Vor- und Frühgeschichtliche Archäologie Rheinische Friedrich-Wilhelms-Universität Bonn, Bonn, pp. 21–26.

Huang, W., Chang, S.-Q., Xie, C.-L., Zhang, Z.-P., 2017. Moisture sources of extreme summer precipitation events in North Xinjiang and their relationship with atmospheric circulation. Advances in Climate Change Research 8, 12–17. doi:10.1016/j.accre.2017.02.001

Iovita, R., Varis, A., Namen, A., Cuthbertson, P., Taimagambetov, Z., Miller, C.E., 2020. In search of a Paleolithic Silk Road in Kazakhstan. Quaternary International 1–14. doi:10.1016/j.quaint.2020.02.023

Ito, T.Y., Tsuge, M., Lhagvasuren, B., Buuveibaatar, B., Chimeddorj, B., Takatsuki, S., Tsunekawa, A., Shinoda, M., 2013. Effects of interannual variations in environmental conditions on seasonal range selection by Mongolian gazelles. Journal of Arid Environments 91, 61–68. doi:10.1016/j.jaridenv.2012.12.008

Janz, L., Odsuren, D., Bukhchuluun, D., 2017. Transitions in Palaeoecology and Technology: Hunter-Gatherers and Early Herders in the Gobi Desert. Journal of World Prehistory 30, 1–80. doi:10.1007/s10963-016-9100-5

Jiang, H., Feng, G., Liu, X., Cao, H., Wang, S., Ma, L., Ferguson, D.K., 2018. Drilling wood for fire: discoveries and studies of the fire-making tools in the Yanghai cemetery of ancient Turpan, China. Vegetation History and Archaeobotany 27, 197–206. doi:10.1007/s00334-017-0611-5

Kaczensky, P., Dresley, V., Vetter, D., Otgonbayar, H., Walzer, C., 2010. Water use of Asiatic wild asses in the Mongolian Gobi. Erforschung biologischer Ressourcen der Mongolei / Exploration into the Biological Resources of Mongolia 11, 291–298.

Kaseke, K.F., Wang, L., Seely, M.K., 2017. Nonrainfall water origins and formation mechanisms. Science Advances 3, 1–9. doi:10.1126/sciadv.1603131

Khatsenovich, A.M., Rybin, E.P., Olsen, J.W., Gunchinsuren, B., Bazargur, D., Marchenko, D.V., Klementiev, A.M., Kogai, S.A., Shelepaev, R.A., Popov, A.Y., Kravtsova, A.S., Shevchenko, T.A., 2018. Chronostratigraphy of the Orkhon-1 Middle Paleolithic Site in Central Mongolia. Problems of Archaeology, Ethnography, Anthropology of Siberia and Neighboring Territories 24, 174–178. doi:10.17746/2658-6193.2018.24.174-178

Khatsenovich, A.M., Rybin, E.P., Bazargur, D., Marchenko, D. V., Kogai, S.A., Shevchenko, T.A., Klementiev, A.M., Gunchinsuren, B., Olsen, J.W., 2019.

Middle Palaeolithic human dispersal in Central Asia: new archaeological investigations in the Orkhon Valley, Mongolia. Antiquity 93, e20. doi:10.15184/aqy.2019.111

Klinge, M., Sauer, D., 2019. Spatial pattern of Late Glacial and Holocene climatic and environmental development in Western Mongolia - A critical review and synthesis. Quaternary Science Reviews 210, 26–50. doi:10.1016/j.quascirev.2019.02.020

Komatsu, G., Olsen, J.W., 2002. Geological and archaeological exploration of caves in Mongolia. Cave and Karst Science 29, 75–86.

Kostrova, S.S., Meyer, H., Bailey, H.L., Ludikova, A. V., Gromig, R., Kuhn, G., Shibaev, Y.A., Kozachek, A. V., Ekaykin, A.A., Chapligin, B., 2019. Holocene hydrological variability of Lake Ladoga, northwest Russia, as inferred from diatom oxygen isotopes. Boreas 48, 361–376. doi:10.1111/bor.12385

Krause, J., Orlando, L., Serre, D., Viola, B., Prüfer, K., Richards, M.P., Hublin, J.-J., Hänni, C., Derevianko, A.P., Pääbo, S., 2007. Neanderthals in central Asia and Siberia. Nature 449, 902–904. doi:10.1038/nature06193

Krause, J., Fu, Q., Good, J.M., Viola, B., Shunkov, M. V., Derevianko, A.P., Pääbo, S., 2010. The complete mitochondrial DNA genome of an unknown hominin from southern Siberia. Nature 464, 894–897. doi:10.1038/nature08976

Kröner, A., Windley, B.F., Badarch, G., Tomurtogoo, O., Hegner, E., Jahn, B.M., Gruschka, S., Khain, E.V., Demoux, A., Wingate, M.T.D., 2007. Accretionary growth and crust formation in the Central Asian Orogenic Belt and comparison with the Arabian-Nubian shield. pp. 181–209. doi:10.1130/2007.1200(11)

Kwang-jin, Y., Tseveendorj, D., Batbold, N., Tsengel, M., Jargalan, B., Lee, S., Im, S.-K., Young, K.H., Ji, J.H., Yang, H.H. (Eds.), 2010a. Shandyn Amny Avst rock burial (In Korean & Mongolian). In: Mongolian Cultural Heritage Studies. Vol 1. National Research Institute of Cultural Heritage in Korea & Institute of Archaeology, Mongolian Academy of Sciences, Seoul, South Korea, pp. 154–165.

Kwang-jin, Y., Tseveendorj, D., Batbold, N., Tsengel, M., Jargalan, B., Lee, S., Im, S.-K., Young, K.H., Ji, J.H., Yang, H.H. (Eds.), 2010b. Tsagaan Gol (In Korean & Mongolian). In: Mongolian cultural heritage studies. Vol 1. National Research Institute of Cultural Heritage in Korea & Institute of Archaeology, Mongolian Academy of Sciences, Seoul, South Korea, pp. 150–153.

Lachniet, M.S., 2009. Climatic and environmental controls on speleothem oxygen-isotope values. Quaternary Science Reviews 28, 412–432. doi:10.1016/j.quascirev.2008.10.021

Lamb, M.A., Badarch, G., 1997. Paleozoic Sedimentary Basins and Volcanic-Arc Systems of Southern Mongolia: New Stratigraphic and Sedimentologic Constraints. International Geology Review 39, 542–576. doi:10.1080/00206819709465288

Landais, A., Risi, C., Bony, S., Vimeux, F., Descroix, L., Falourd, S., Bouygues, A., 2010. Combined measurements of 17Oexcess and d-excess in African monsoon precipitation: Implications for evaluating convective parameterizations. Earth and Planetary Science Letters 298, 104–112. doi:10.1016/j.epsl.2010.07.033

Lehmkuhl, F., 2015. Modern and past periglacial features in Central Asia and their implication for paleoclimate reconstructions. Progress in Physical Geography 40, 369–391. doi:10.1177/0309133315615778

Lehmkuhl, F., Stauch, G., Batkhishig, O., 2003. Rock glacier and periglacial processes in the Mongolian Altai. In: Phillips, M., Springman, S.M., Arenson, L.U. (Eds.), Proceeding of the 8th International Conference on Permafrost, 21-25 2003, Zürich, Switzerland. Zürich, pp. 639–644.

Lehmkuhl, F., Nottebaum, V., Hülle, D., 2018. Aspects of late Quaternary geomorphological development in the Khangai Mountains and the Gobi Altai Mountains (Mongolia). Geomorphology 312, 24–39. doi:10.1016/j.geomorph.2018.03.029

Li, F., Kuhn, S.L., Chen, F., Wang, Y., Southon, J., Peng, F., Shan, M., Wang, C., Ge, J., Wang, X., Yun, T., Gao, X., 2018. The easternmost Middle Paleolithic (Mousterian) from Jinsitai Cave, North China. Journal of Human Evolution 114, 76–84. doi:10.1016/j.jhevol.2017.10.004

Li, F., Vanwezer, N., Boivin, N., Gao, X., Ott, F., Petraglia, M., Roberts, P., 2019. Heading north: Late Pleistocene environments and human dispersals in central and eastern Asia. PLOS ONE 14, e0216433. doi:10.1371/journal.pone.0216433

Li, S.-G., Romero-Saltos, H., Tsujimura, M., Sugimoto, A., Sasaki, L., Davaa, G., Oyunbaatar, D., 2007. Plant water sources in the cold semiarid ecosystem of the upper Kherlen River catchment in Mongolia: A stable isotope approach. Journal of Hydrology 333, 109–117. doi:10.1016/j.jhydrol.2006.07.020

Lkhagvadorj, D., Hauck, M., Dulamsuren, C., Tsogtbaatar, J., 2013. Pastoral nomadism in the forest-steppe of the Mongolian Altai under a changing economy and a warming climate. Journal of Arid Environments 88, 82–89. doi:10.1016/j.jaridenv.2012.07.019

Lkhamjav, J., Jin, H.-G., Lee, H., Baik, J.-J., 2017. A hail climatology in Mongolia. Asia-Pacific Journal of Atmospheric Sciences 53, 501–509. doi:10.1007/s13143-017-0052-1

Louys, J., Kealy, S., O’Connor, S., Price, G., Hawkins, S., Aplin, K., Rizal, Y., Zaim, J., Mahirta, Tanudirjo, D., Santoso, W.D., Hidayah, A.R., Trihascaryo, A., Wood, R., Bevitt, J., Clark, T., 2017. Differential preservation of vertebrates in Southeast Asian caves. International Journal of Speleology 46, 379–408. doi:10.5038/1827-806X.46.3.2131

Lundberg, J., Noiriel, C., Noguès, X., 2008. Expedition speleologique en Mongolie. Bordeaux.

Luz, B., Barkan, E., 2010. Variations of 17O/16O and 18O/16O in meteoric waters. Geochimica et Cosmochimica Acta 74, 6276–6286. doi:10.1016/j.gca.2010.08.016

Malatesta, L.C., Avouac, J.-P., Brown, N.D., Breitenbach, S.F.M., Pan, J., Chevalier, M.-L., Rhodes, E., Saint-Carlier, D., Zhang, W., Charreau, J., Lavé, J., Blard, P.-H., 2018. Lag and mixing during sediment transfer across the Tian Shan piedmont caused by climate-driven aggradation-incision cycles. Basin Research 30, 613–635. doi:10.1111/bre.12267

Marchenko, D. V., Khatsenovich, A.M., Rybin, E.P., Bazargur, D., Byambaa, G., Olsen, J.W., 2020. Comparison Study of Cultural Layers Preservation at the Moiltyn Am Site (Central Mongolia). Vestnik NSU. Series: History and Philology 19, 70–85. doi:10.25205/1818-7919-2020-19-5-70-85

Marchina, C., Lepetz, S., Salicis, C., Magail, J., 2017. The skull on the hill. Anthropological and osteological investigation of contemporary horse skull ritual practices in central Mongolia (Arkhangai province). Anthropozoologica 52, 171–183. doi:10.5252/az2017n2a3

Martynovich, N., 2002. Pleistocene birds from Tsagan-Agui cave (Gobian Altai). Acta Zoologica Cracoviensia 45, 283–292.

Massilani, D., Skov, L., Hajdinjak, M., Gunchinsuren, B., Tseveendorj, D., Yi, S., Lee, J., Nagel, S., Nickel, B., Devièse, T., Higham, T., Meyer, M., Kelso, J., Peter, B.M., Pääbo, S., 2020. Denisovan ancestry and population history of early East Asians. Science 370, 579–583. doi:10.1126/science.abc1166

Meyer, M., Kircher, M., Gansauge, M.-T., Li, H., Racimo, F., Mallick, S., Schraiber, J.G., Jay, F., Prufer, K., Filippo, C. de, Sudmant, P.H., Alkan, C., Fu, Q., Do, R., Rohland, N., Tandon, A., Siebauer, M., Green, R.E., Bryc, K., Briggs, A.W., Stenzel, U., Dabney, J., Shendure, J., Kitzman, J., Hammer, M.F., Shunkov, M. V., Derevianko, A.P., Patterson, N., Andres, A.M., Eichler, E.E., Slatkin, M., Reich, D., Kelso, J., Paabo, S., 2012. A High-Coverage Genome Sequence from an Archaic Denisovan Individual. Science 338, 222–226. doi:10.1126/science.1224344

Miller, B.K., 2012. Vehicles of the steppe elite: chariots and carts in Xiongnu tombs. The Silk Road 10, 29–38.

Monteith, F., 2017. Towards a landscape archaeology of Buddhist cave-temples in China. Antiquity 91, e8. doi:10.15184/aqy.2017.169

Munkherdene, G., Sneath, D., 2018. Enclosing the Gold-Mining Commons of Mongolia: The Vanishing Ninja and the Development Project as Resource. Current Anthropology 59, 814–838. doi:10.1086/700961

Munkhtsetseg, E., Kimura, R., Wang, J., Shinoda, M., 2007. Pasture yield response to precipitation and high temperature in Mongolia. Journal of Arid Environments 70, 94–110. doi:10.1016/j.jaridenv.2006.11.013

Munkhtsog, B., Purevjav, L., McCarthy, T., Bayrakçısmith, R., 2016. Northern Range: Mongolia. In: McCarthy, T., Mallon, D. (Eds.), Snow Leopards. Elsevier, pp. 493–500. doi:10.1016/B978-0-12-802213-9.00039-0

Murdoch, J.D., Reading, R.P., Amgalanbaatar, S., Wingard, G., Lkhagvasuren, B., 2017. Ecological interactions shape the distribution of a cultural ecosystem service: Argali sheep (Ovis ammon) in the Gobi-Steppe of Mongolia. Biological Conservation 209, 315–322. doi:10.1016/j.biocon.2017.02.035

Nomguunsuren, G., Ahrens, B., Piezonka, H., 2012. Das Höhlengrab von Cagaan Chad, Bogd sum, Övörchangaj ajmag. In: Steppenkrieger: Reiternomaden Des 7. - 14. Jahrhunderts Aus Der Mongolei. pp. 325–349.

O'Regan, H., Kuman, K., Clarke, J.R., 2011. The likely accumulators of bones: five cape porcupine den assembalges and the role of porcupines in the post-Member 6 infill at Sterkfontein, south Africa. Journal of taphonomy 9, 69–87.

Olsen, J.W., 2003. The Paleolithic archaeology of North Central Mongolia: 2002 Field Report. Tuscon.

Owen, L.A., Wittwer, C.T., Cunningham, W.D., Badamgarav, J., Dorjnamjaa, D., Windley, B.F., Cunningham, W.D., Badamgarav, J., Dorjnamjaa, D., 1997. Quaternary alluvial fans in the Gobi of southern Mongolia: evidence for neotectonics and climate change. Journal of Quaternary Science 12, 239–252. doi:10.1002/(SICI)1099-1417(199705/06)12:3<239::AID-JQS293>3.0.CO;2-P

Owen, L.A., Richards, B., Rhodes, E.J., Cunningham, W.D., Windley, B.F., Badamgarav, J., Dorjnamjaa, D., 1998. Relic permafrost structures in the Gobi of Mongolia: age and significance. Journal of Quaternary Science 13, 539–547. doi:10.1002/(SICI)1099-1417(1998110)13:6<539::AID-JQS390>3.0.CO;2-N

Owen, L.A., Cunningham, D., Richards, B.W.M., Rhodes, E., Windley, B.F., Dorjnamjaa, D., Badamgarav, J., 1999. Timing of formation of forebergs in the northeastern Gobi Altai, Mongolia: implications for estimating mountain uplift rates and earthquake recurrence intervals. Journal of the Geological Society

156, 457–464. doi:10.1144/gsjgs.156.3.0457

Payne, J.C., Buuveibaatar, B., Bowler, D.E., Olson, K.A., Walzer, C., Kaczensky, P., 2020. Hidden treasure of the Gobi: understanding how water limits range use of khulan in the Mongolian Gobi. Scientific Reports 10, 2989. doi:10.1038/s41598-020-59969-2

Pearson, K.R., Mönkhbayar, C., Enkhbat, G., Bayarsaikhan, J., 2019. The Textiles of Üzüür Gyalan: Towards the identification of a nomadic weaving tradition in the Mongolian Altai. Archaeological Textiles Review 53, 1689–1699. doi:10.1017/CBO9781107415324.004

Peel, M.C., Finlayson, B.L., McMahon, T.A., 2007. Updated world map of the Köppen-Geiger climate classification. Hydrology and Earth System Sciences 11, 1633–1644. doi:10.5194/hess-11-1633-2007

Ritz, J.-F., Bourlès, D., Brown, E.T., Carretier, S., Chéry, J., Enhtuvshin, B., Galsan, P., Finkel, R.C., Hanks, T.C., Kendrick, K.J., Philip, H., Raisbeck, G., Schlupp, A., Schwartz, D.P., Yiou, F., 2003. Late Pleistocene to Holocene slip rates for the Gurvan Bulag thrust fault (Gobi-Altay, Mongolia) estimated with 10 Be dates. Journal of Geophysical Research: Solid Earth 108, 1–16. doi:10.1029/2001JB000553

Rother, H., Lehmkuhl, F., Fink, D., Nottebaum, V., 2014. Surface exposure dating reveals MIS-3 glacial maximum in the Khangai Mountains of Mongolia. Quaternary Research (United States) 82, 297–308. doi:10.1016/j.yqres.2014.04.006

Rybin, E.P., Khatsenovich, A.M., Zwyns, N., Gunchinsuren, B., Paine, C.H., Bolorbat, T., Anoikin, A.A., Kharevich, V.M., Odsuren, D., Margad-Eredene, G., 2017. Stratigraphy and Cultural Sequence of the Tolbor 21 Site (Northern

Mongolia): the Results of the 2014–2016 Excavation Campaigns and Perspectives of Further Investigations [Russian]. Teoriya i praktika arkheologicheskikh issledovaniy 20, 158–168. doi:10.14258/tpai(2017)4(20).-12

Rybin, E.P., Paine, C.H., Khatsenovich, A.M., Tsedendorj, B., Talamo, S., Marchenko, D. V., Rendu, W., Klementiev, A.M., Odsuren, D., Gillam, J.C., Gunchinsuren, B., Zwyns, N., 2020. A new Upper Paleolithic occupation at the site of Tolbor-21 (Mongolia): Site formation, human behavior and implications for the regional sequence. Quaternary International 21. doi:10.1016/j.quaint.2020.06.022

Schoenemann, S.W., Schauer, A.J., Steig, E.J., 2013. Measurement of SLAP and GISP δ17O and proposed VSMOW-SLAP normalization for δ17O and 17O-excess. Rapid Communications in Mass Spectrometry 27, 582–590.

Slon, V., Viola, B., Renaud, G., Gansauge, M.-T., Benazzi, S., Sawyer, S., Hublin, J.-J., Shunkov, M. V., Derevianko, A.P., Kelso, J., Prüfer, K., Meyer, M., Pääbo, S., 2017a. A fourth Denisovan individual. Science Advances 3, e1700186. doi:10.1126/sciadv.1700186

Slon, V., Hopfe, C., Weiß, C.L., Mafessoni, F., la Rasilla, M. de, Lalueza-Fox, C., Rosas, A., Soressi, M., Knul, M. V., Miller, R., Stewart, J.R., Derevianko, A.P., Jacobs, Z., Li, B., Roberts, R.G., Shunkov, M. V., Lumley, H. de, Perrenoud, C., Gušić, I., Kućan, Ž., Rudan, P., Aximu-Petri, A., Essel, E., Nagel, S., Nickel, B., Schmidt, A., Prüfer, K., Kelso, J., Burbano, H.A., Pääbo, S., Meyer, M., 2017b. Neandertal and Denisovan DNA from Pleistocene sediments. Science 9695, eaam9695. doi:10.1126/science.aam9695

Sponheimer, M., Lee-Thorp, J.A., 1999. Oxygen Isotopes in Enamel Carbonate and their Ecological Significance. Journal of Archaeological Science 26, 723–728.

doi:10.1006/jasc.1998.0388

Steig, E.J., Gkinis, V., Schauer, A.J., Schoenemann, S.W., Samek, K., Hoffnagle, J., Dennis, K.J., Tan, S.M., 2014. Calibrated high-precision 17O-excess measurements using cavity ring-down spectroscopy with laser-current-tuned cavity resonance. Atmospheric Measurement Techniques 7, 2421–2435. doi:10.5194/amt-7-2421-2014

Stein, A.F., Draxler, R.R., Rolph, G.D., Stunder, B.J.B., Cohen, M.D., Ngan, F., 2015. NOAA's HYSPLIT Atmospheric Transport and Dispersion Modeling System. Bulletin of the American Meteorological Society 96, 2059–2077. doi:10.1175/BAMS-D-14-00110.1

Straus, L.G., 1990. Underground Archaeology: perspectives on caves and rockshelters. Archaeological Method and Theory 2, 255–304.

Taylor, W., Shnaider, S., Abdykanova, A., Fages, A., Welker, F., Irmer, F., Seguin-Orlando, A., Khan, N., Douka, K., Kolobova, K., Orlando, L., Krivoshapkin, A., Boivin, N., 2018. Early pastoral economies along the Ancient Silk Road: Biomolecular evidence from the Alay Valley, Kyrgyzstan. PLOS ONE 13, e0205646. doi:10.1371/journal.pone.0205646

Taylor, W.T.T., Clark, J., Bayarsaikhan, J., Tuvshinjargal, T., Jobe, J.T., Fitzhugh, W., Kortum, R., Spengler, R.N., Shnaider, S., Seersholm, F.V., Hart, I., Case, N., Wilkin, S., Hendy, J., Thuering, U., Miller, B., Miller, A.R.V., Picin, A., Vanwezer, N., Irmer, F., Brown, S., Abdykanova, A., Shultz, D.R., Pham, V., Bunce, M., Douka, K., Jones, E.L., Boivin, N., 2020. Early Pastoral Economies and Herding Transitions in Eastern Eurasia. Scientific Reports 10, 1001. doi:10.1038/s41598-020-57735-y

Terguunbayar, A.S., Ankhsanaa, K.K., 2019. Rock Art in Mongolia. In: Clottes, J.,

Journal Pre-proof

Smith, B. (Eds.), Rock Art in East Asia: A Thematic Study. ICOMOS International, Paris.

Tian, C., Wang, L., Tian, F., Zhao, S., Jiao, W., 2019. Spatial and temporal variations of tap water 17O-excess in China. Geochimica et Cosmochimica Acta 260, 1–14. doi:10.1016/j.gca.2019.06.015

Törbat, T., Batsükh, D., Bemmann, J., Höllmann, T.O., Zieme, P., 2009. A Rock Tomb of the Ancient Turkic Period in the Zhargalant Khairkhan Mountains, Khovd Aimag, With the Oldest Preserved Horse-Head Fiddle in Mongolia – A Preliminary Report. In: Bemmann, J., Parzinger, H., Pohl, E., Tseveendorzh, D. (Eds.), Current Archaeological Research in Mongolia. Vor- und Frühgeschichtliche Archäologie Rheinische Friedrich-Wilhelms-Universität Bonn, Bonn, pp. 365–383.

Tumendemberel, O., Proctor, M., Reynolds, H., Boulanger, J., Luvsamjamba, A., Tserenbataa, T., Batmunkh, M., Craighead, D., Yanjin, N., Paetkau, D., 2015. Gobi bear abundance and inter-oases movements, Gobi Desert, Mongolia. Ursus 26, 129. doi:10.2192/URSUS-D-15-00001.1

Turner, B.L., Zuckerman, M.K., Garofalo, E.M., Wilson, A., Kamenov, G.D., Hunt, D.R., Amgalantugs, T., Frohlich, B., 2012. Diet and death in times of war: isotopic and osteological analysis of mummified human remains from southern Mongolia. Journal of Archaeological Science 39, 3125–3140. doi:10.1016/j.jas.2012.04.053

Uechi, Y., Uemura, R., 2019. Dominant influence of the humidity in the moisture source region on the 17O-excess in precipitation on a subtropical island. Earth and Planetary Science Letters 513, 20–28. doi:10.1016/j.epsl.2019.02.012

Vaks, A., Gutareva, O.S., Breitenbach, S.F.M., Avirmed, E., Mason, A.J., Thomas, A.L., Osinzev, A. V., Kononov, A.M., Henderson, G.M., 2013. Speleothems Reveal 500,000-Year History of Siberian Permafrost. Science 340, 183–186. doi:10.1126/science.1228729

Vaks, A., Mason, A.J., Breitenbach, S.F.M., Kononov, A.M., Osinzev, A. V., Rosensaft, M., Borshevsky, A., Gutareva, O.S., Henderson, G.M., 2020. Palaeoclimate evidence of vulnerable permafrost during times of low sea ice. Nature 577, 221–225. doi:10.1038/s41586-019-1880-1

Vanwezer, N., Taylor, W., Jamsranjav, B., Breitenbach, S.F.M., Amano, N., Louys, J., Val, M. del, Boivin, N., Petraglia, M., 2020. Hunting, herding, and people in the rock art of Mongolia: New discoveries in the Gobi-Altai Mountains. Archaeological Research in Asia In Review.

Vassallo, R., Ritz, J.-F., Braucher, R., Carretier, S., 2005. Dating faulted alluvial fans with cosmogenic 10Be in the Gurvan Bogd mountain range (Gobi-Altay, Mongolia): climatic and tectonic implications. Terra Nova 17, 278–285. doi:10.1111/j.1365-3121.2005.00612.x

Vassallo, R., Ritz, J.-F., Carretier, S., 2011. Control of geomorphic processes on 10Be concentrations in individual clasts: Complexity of the exposure history in Gobi-Altay range (Mongolia). Geomorphology 135, 35–47. doi:10.1016/j.geomorph.2011.07.023

Vaurie, C., 1964. A survey of the birds of Mongolia. American Museum of Natural History, New York.

Wal, J.L.N. van der, Nottebaum, V.C., Gailleton, B., Stauch, G., Weismüller, C., Batkhishig, O., Lehmkuhl, F., Reicherter, K., 2020. Morphotectonics of the northern Bogd fault and implications for Middle Pleistocene to modern uplift rates in southern Mongolia. Geomorphology 155, 107330.

doi:10.1016/j.geomorph.2020.107330

Wang, X.M., Flynn, L.J., Fortelius, M., 2013. Toward a continental Asian biostratigraphic and geochronologic framework. In: Wang, X.M., Flynn, L.J., Fortelius, M. (Eds.), Fossil Mammals of Asia: Neogene Biostratigraphy and Chronology. Columbia University Press, New York, pp. 1–28.

Wright, J., 2016. Households without Houses: Mobility and Moorings on the Eurasian Steppe. Journal of Anthropological Research 72, 133–157. doi:10.1086/686297

Yamanaka, T., Tsujimura, M., Oyunbaatar, D., Davaa, G., 2007. Isotopic variation of precipitation over eastern Mongolia and its implication for the atmospheric water cycle. Journal of Hydrology 333, 21–34. doi:10.1016/j.jhydrol.2006.07.022

Yanshin, A.L., Zaitsev, N.S., Kovalenko, V.I., Luvsandanzan, B., Luchitsky, I.V., Yarmolyuk, V.V., 1989. Map of the geological formations of the Mongolian People’s Republic. Scale 1:1500000 (in Russian), Academa Nauka. Moscow.

Zhang, D., Xia, H., Chen, F., Li, B., Slon, V., Cheng, T., Yang, R., Jacobs, Z., Dai, Q., Massilani, D., Shen, X., Wang, J., Feng, X., Cao, P., Yang, M.A., Yao, J., Yang, J., Madsen, D.B., Han, Y., Ping, W., Liu, F., Perreault, C., Chen, X., Meyer, M., Kelso, J., Pääbo, S., Fu, Q., 2020. Denisovan DNA in Late Pleistocene sediments from Baishiya Karst Cave on the Tibetan Plateau. Science 370, 584–587. doi:10.1126/science.abb6320

Zhao, L., Wu, Q., Marchenko, S.S., Sharkhuu, N., 2010. Thermal state of permafrost and active layer in Central Asia during the international polar year. Permafrost and Periglacial Processes 21, 198–207. doi:10.1002/ppp.688

Zhu, H., Wang, D., Wang, L., Fang, J., Sun, W., Ren, B., 2014. Effects of altered precipitation on insect community composition and structure in a meadow steppe. Ecological Entomology 39, 453–461. doi:10.1111/een.12120

Zwyns, N., Gladyshev, S.A., Gunchinsuren, B., Bolorbat, T., Flas, D., Dogandžić, T., Tabarev, A. V., Gillam, J.C., Khatsenovich, A.M., McPherron, S., Odsuren, D., Paine, C.H., Purevjal, K.-E., Stewart, J.R., 2014. The open-air site of Tolbor 16 (Northern Mongolia): Preliminary results and perspectives. Quaternary International 347, 53–65. doi:10.1016/j.quaint.2014.05.043

Zwyns, N., Paine, C.H., Tsedendorj, B., Talamo, S., Fitzsimmons, K.E., Gantumur, A., Guunii, L., Davakhuu, O., Flas, D., Dogandžić, T., Doerschner, N., Welker, F., Gillam, J.C., Noyer, J.B., Bakhtiary, R.S., Allshouse, A.F., Smith, K.N., Khatsenovich, A.M., Rybin, E.P., Byambaa, G., Hublin, J.-J., 2019. The Northern Route for Human dispersal in Central and Northeast Asia: New evidence from the site of Tolbor-16, Mongolia. Scientific Reports 9, 11759. doi:10.1038/s41598-019-47972-1

Fig. 1. Map of recorded Mongolian caves. The four red boxes mark regions surveyed as part of this paper: (A) Tsakhiryn Nuruu. (B) Aguin Nuruu. (C) Gazar region (D) Saalit region and Chikhen Agui. See Fig. 4 for insets

Fig. 2 Mean monthly precipitation and temperature at the Altai meteorological station. Both precipitation (P) and temperature (T) show strong seasonality, with maxima during summer. The percentiles ranges (colour shading) highlight pronounced interannual variability of summer rainfall and winter temperatures. Data source: https://climexp.knmi.nl, last access 17.04.2020.

Fig. 3 Karstifiable rock types in the surrounding of the Gobi-Altai, with study regions discussed in the main text highlighted with red inserts. Geological information modified from Yanshin et al. (1989).

Fig. 4. Cave locations found through surveys and relevant water bodies. A. Gorge of Tsakhiryn Nuruu. B. Gorge of Aguin Nuruu. C. Gazar hills. D. Saalit caves and Chikhen Agui. Sites labelled are: 1. Tsakhiryn Agui 1, 2. Tsakhiryn Agui 1b, 3. Tsakhiryn Agui 2, 4. Tsakhiryn Agui 3, 5. Tsakhiryn Agui 4, 6. Tsakhiryn Agui 5, 7. Irvesiin Agui, 8. Nuramt Tsakhir Agui, 9. Khongil Tsakhir Agui, 10-22. Gazar Agui 1-13, 23. Saalit Agui 1, 24. Saalit Agui 2, 25. Saalit Agui 3 26. Chikhen Agui – See Table 1 for individual coordinates.

Fig. 5 A. Plan, profile and section drawings of Tsakhiryn Agui. B. Large debris cone that leads to entrances of 3 caves (credit: S. Breitenbach). C. Entrance to Tsakhiryn Agui 1, with sampling gear for scale (credit: A. Kononov).

Fig. 6 Organic finds from Tsakhiryn Agui. A. Fragmented wood beam (TSA-2018-200001), B. Possible wooden whip handle (TSA-2018-200011), C. Fragment of ger lattice (TSA-2018-200002), D. First locus, wood tools in cave floor crevice (8 cm lens cap for scale) E. Second locus, wood tools.

Fig. 7 Organic finds from Tsakhiryn Agui. A. Fragment of bow drill (TSA-2018-200004). B. Unused fragmented of fire-starting hearth (TSA-2018-200006), notches are preparations to allow embers to fall into tinder C. Complete fire drill (TSA-2018-200020), flattened end goes onto the hearth to create friction, and sharpened end would be placed in handhold.

Fig. 8 A. Plan and cross section drawings of Tsakhiryn Agui 4, Red rectangle marks the excavated area. B. Escarpment towards entrance of Tsakhiryn Agui

Fig. 9 A. Plan and profile of Irvesiin Agui, with labelled sampling locations. B. Entrance to Irvesiin Agui. C. Speleothem (flowstone) deposit recovered from Irvesiin Agui. Translucent calcite layers, intercalated with brownish/yellowish detrital layers, are deposited sub-horizontally on brecciated reddish-white cave sediment. D. Crystal sand sample consisting of potassium nitrate

Fig. 10 Plan and profile drawings of Nuramt Tsakhir Agui with red square outlining excavation area.

Fig. 11 A. Cave plan and profile of Khongil Tsakhir Agui, with labels of specific photos and references. B. View of limestone cliff that contains Khongil Tsakhir Agui, with people at top for scale. C. View of entrance with Tibetan Buddhist mantra engraved on the left (white square). D. Skull of *Equus* sp. found in the main chamber. E. Main vertical tunnel of cave. F. One of southern entrances to cave. G. Divide between two tunnels. H. Two south facing circular windows. I. Miniature Buddhist stupa in smaller tunnel.

Fig. 12 A. Cave plan and profile of Gazar Agui 1 with the excavation indicated in red. 1-7 indicate the location of seven petroglyphs. B. View of Gazar Agui 1 entrance, ovicaprid dung floor, and the wall made of cave spall. C. Lithic findings from Gazar Agui 1. i. proximal microblade fragment. ii. medial microblade fragment. iii. backed microblade fragment. iv. medial microblade fragment. v. medial microblade fragment. D. Western section of trench, red dots denoting location of radiocarbon samples taken, white lines demarcate divisions of layers. E. Northern section of trench with samples taken and micromorphology sample.

Fig. 13 Gazar Agui 13 cave profile and plan, with red rectangles indicating the excavated area and points indicating location of petroglyphs.

Fig. 14 Overview of available stable isotope ($\delta^{18}O$ and δD) data from Mongolia. Samples presented here are consistent with those observed by Yamanaka et al. (2007) indicating a common history. See SI Fig. 1 for their geographic distribution. Data from south of the Gobi-Altai ranges (published by Burnik šturm et al. 2015, 2017), however, show distinct slopes and intercepts, pointing to very arid moisture sources affected by significant secondary evaporation. The Gobi-Altai region thus shows two distinct moisture dynamics.

Fig. 15 The negative correlation observed between $\delta^{18}O$ and $^{17}O_{excess}$ in waters from NW Mongolia (this study) suggests that secondary evaporation during summer is traceable in the water isotope signal. Filled blue circles show river samples, open circles indicate rainwater samples, and filled orange circles show dripwaters. Errors indicate one standard error (1 SE) of the individual analyses.

Fig. 16 Summary of $\delta^{18}O$ vs. d-excess data for Mongolian waters. Low $\delta^{18}O$ and high d-excess values are indicative of a high-humidity/low temperature moisture source. High $\delta^{18}O$ values and low d-excess values (<0) are indicative of increasing importance of secondary re-evaporation under very arid conditions. Very low $\delta^{18}O$ values indicate winter snow delivered from western sources. Samples from north of the Altai are sourced from a more humid region and show much less secondary evaporation compared to those sampled southwest of the Gobi-Altai Mountain Range which originate from hyper-arid regions.

Table 1. Sites recorded in this paper

Table 2. Visual analysis of wood pieces from Tsakhiryn Agui 1

Table 3. Radiocarbon dating of wood pieces Tsakhiryn Agui 1

Table 4. Radiocarbon dating of burned sediments from Gazar Agui 1

Site Name	Soum (district)	Longitude E (DD) WGS84	Latitude N (DD) WGS84	Elevation m a.s.l. (uncal)	Excavation	Breccia
Tsakhiryn Agui 1	Khaliun	96.28559	45.845921	1904		
Tsakhiryn Agui 1b	Khaliun	96.28559	45.845921	1890		
Tsakhiryn Agui 2	Khaliun	96.27474	45.849919	2007		
Tsakhiryn Agui 3	Khaliun	96.27557	45.849911	2024		
Tsakhiryn Agui 4	Khaliun	96.28183	45.854959	2054	x	
Tsakhiryn Agui 5	Khaliun	96.27914	45.853443	2056		
Irvesiin Agui	Khaliun	96.27684	45.853218	2083		x
Nuramt Tsakhir Agui	Khaliun	95.79398	45.878726	2092	x	
Khongil Tsakhir Agui	Khaliun	95.80328	45.878231	2025		
Gazar Agui 1	Taishir	96.2194	46.763898	2026	x	
Gazar Agui 2	Taishir	96.23888	46.692067	2085		
Gazar Agui 3	Taishir	96.23852	46.6921	2094		
Gazar Agui 4	Taishir	96.21839	46.76562	2060		
Gazar Agui 5	Taishir	96.21839	46.76562	2060		
Gazar Agui 6	Taishir	96.21839	46.76562	2060		
Gazar Agui 7	Taishir	96.22803	46.762741	2057		
Gazar Agui 8	Taishir	96.21956	46.764154	2053		
Gazar Agui 9	Taishir	96.21236	46.765564	2067		
Gazar Agui 10	Taishir	96.21236	46.765564	2078		
Gazar Agui 11	Taishir	96.21946	46.764151	2042		
Gazar Agui 12	Taishir	96.21946	46.764151	2042		
Gazar Agui 13	Taishir	96.20794	46.763367	2078	x	
Saalit Agui 1	Bayan-Ondor	99.04367	44.784024	2065		
Saalit Agui 2	Bayan-Ondor	99.04735	44.782081	2052		
Saalit Agui 3	Bayan-Ondor	99.04151	44.786055	2120		

Project-ID	Material	Piece	Observations	Broken?	Break type and location
TSA-2018-200001	wood	beam	2 rectangular holes	yes	both ends and longitudinally
TSA-2018-200002	wood	ger lattice beam	3 circular holes	yes	proximal end
TSA-2018-200003	wood	branch	Distal end slightly sharpened, one branch	yes	proximal end
TSA-2018-200004	wood	bow drill	One end has a nock and a natural knot in centre	yes	one end broken
TSA-2018-200005	wood	board	Unused hearth	yes	longitudinal crack
TSA-2018-200006	wood	hearth	single side with prepared notches	yes	Both ends
TSA-2018-200007	horn (caprine)		3 circular holes (two lateral, one medial)	yes	crack on anterior side
TSA-2018-200008	wood	stick	Possibly drill, one sharpened tapered end	yes	one end broken
TSA-2018-200009	wood	stick	knot	yes	both ends
TSA-2018-200010	wood	curved stick	curved knot on one end, dulled other end	yes	one end broken
TSA-2018-200011	wood	whip	rounded end with hole, tapered and curved other end	no	
TSA-2018-200012	wood	curved stick		yes	both ends broken
TSA-2018-200013	wood	curved stick	rounded ends, several bends	yes	longitudinal crack
TSA-2018-200014	wood	stick	one end sharpened tapered	yes	one end
TSA-2018-200015	wood	drill	rounded end with blackened colour	yes	cracked rounded end, broken other end
TSA-2018-200016	wood	board	circular hole, pointed end	yes	crack by hole, pointed end blunted
TSA-2018-200017	wood	stick		yes	both ends
TSA-2018-200018	wood	stick		yes	both ends and section in middle
TSA-2018-200019	wood	stick	one side rounded	yes	one end broken, rounded end cracked
TSA-2018-200020	wood	drill	rounded end, another sharpened to taper, bark present	yes	latitudinal cut on tapered end
TSA-2018-200021	wood	stick	rounded end	yes	broken end, longitudinal cracks
TSA-2018-200022	wood	curved stick	rounded end, natural end	yes	longitudinal crack on rounded end
TSA-2018-200023	wood	drill	rounded end and sharpened tapered end	yes	small crack on rounded end
TSA-2018-200024	wood	stick	circular hole on one end	yes	fractured on both ends, longitudinal cracks on whole piece
TSA-2018-200025	wood	stick	rounded bulb end, singed on other end	yes	both ends broken
TSA-2018-200026	wood	stick		yes	both ends broken
TSA-2018-200027	wood	stick	Sent for C14	yes	broken in half longitudinally, both ends broken
TSA-2018-200028	wood	stick	Sent for C14, both ends singed	yes	broken in half longitudinally, both ends broken
TSA-2018-200029	wood	hearth	preliminary jagged pattern to create notches	yes	both ends broken, completely cracked
TSA-2018-200030	wood	stick	Rounded end, has bark	yes	one end broken
TSA-2018-200031	wood	board	socket on one end, circular hole	yes	longitudinal cracks
TSA-2018-200032	wood	hearth	notched preparations on one side, not all notches finished	yes	longitudinal crack, broken ends

Project-ID	Lab ID	BP	uncertainty	Cal AD (IntCal20)	uncertainty	probability (95.4%)	material
TSA-2018-200027	OxA-40026	966	±19	1040	±14	23.90%	wood
				1117	±40	71.50%	
TSA-2018-200028	OxA-40027	1760	±19	252	±14	20.60%	wood
				310	±40	74.90%	
	OxA-40028	1766	±19	251	±13	21.70%	wood
				310	±35	73.80%	

Project-ID	Lab ID	BP	uncertainty	cal AD (IntCal20)	uncertainty	probability (95.4%)	material
GZA-2018-100055	OxA-38642	1.11038*	±0.00263				burned soil
GZA-2018-100104	OxA-38701	148	±21	1686	±20	15.30%	burned soil
				1750	±30	26.10%	
				1807	±11	9.90%	
				1862	±30	23.90%	
				>1907		20.20%	
GZA-2018-100101	OxA-38773	1.04737*	±0.00241				burned soil
GZA-2018-100102	OxA-38774	1.03738*	±0.00237				burned soil

*modern date (post 1950) reported as F14C (fraction of modern)

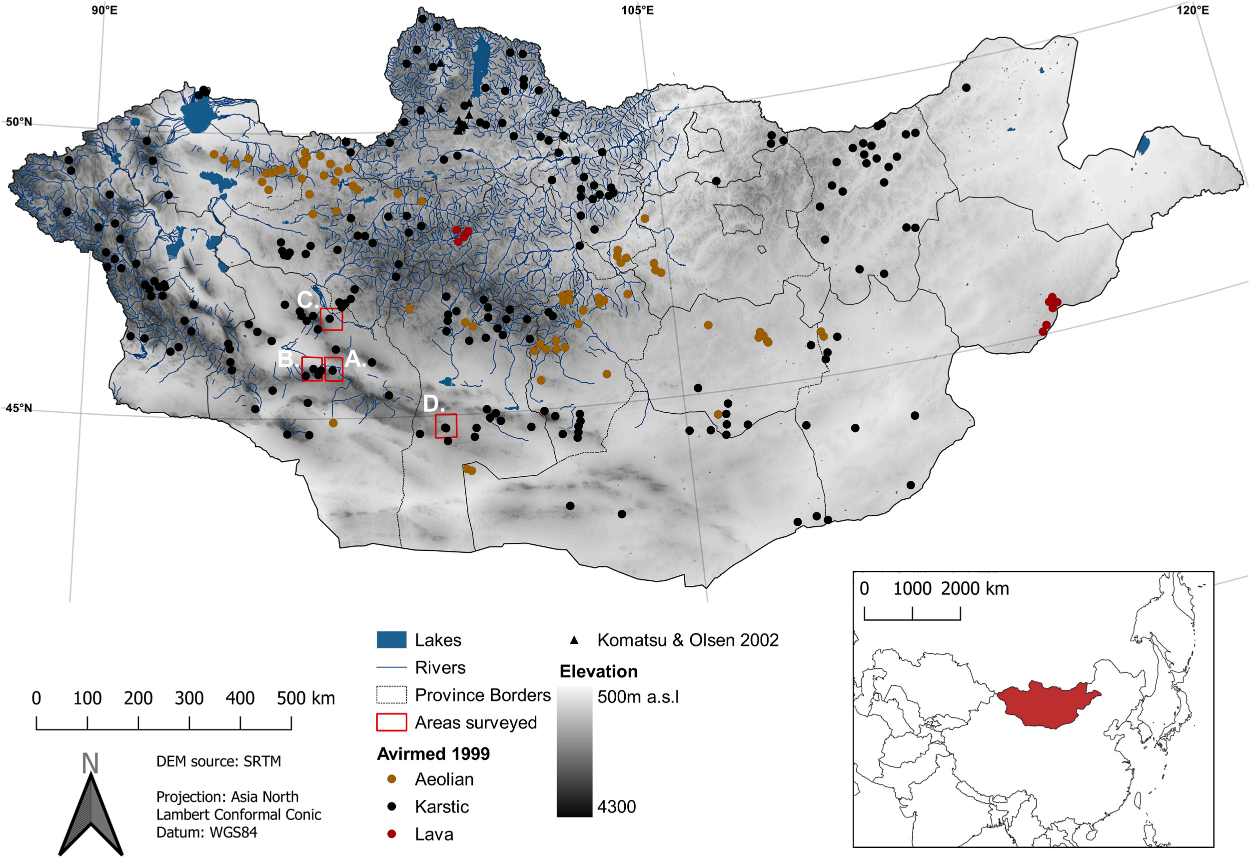
90°E
105°E
120°E
50°N
45°N
C.
B.
A.
D.
0 1000 2000 km
Lakes
Rivers
Province Borders
Areas surveyed
Komatsu & Olsen 2002
Elevation
500m a.s.l
4300
Avirmed 1999
Aeolian
Karstic
Lava
0 100 200 300 400 500 km
N
DEM source: SRTM
Projection: Asia North Lambert Conformal Conic
Datum: WGS84

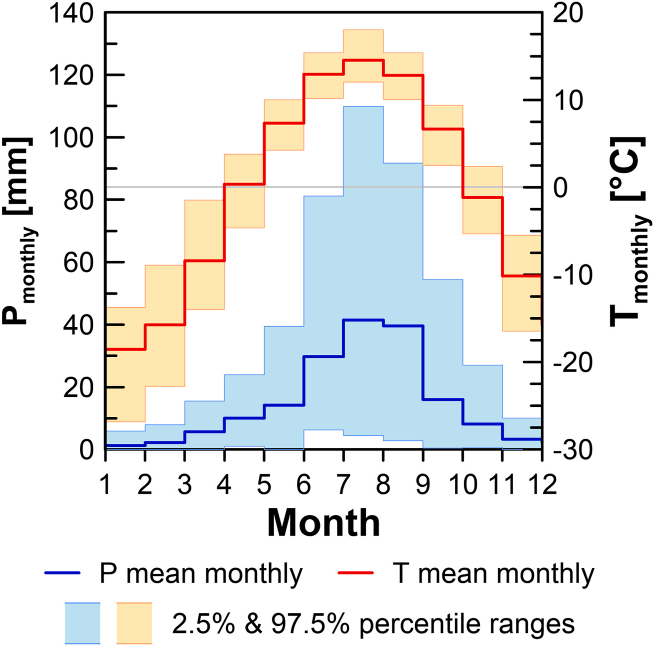

140
120
100
80
60
40
20
0
P monthly [mm]
20
10
0
-10
-20
-30
T monthly [°C]
1
2
3
4
5
6
7
8
9
10
11
12
Month
P mean monthly
T mean monthly
2.5% & 97.5% percentile ranges

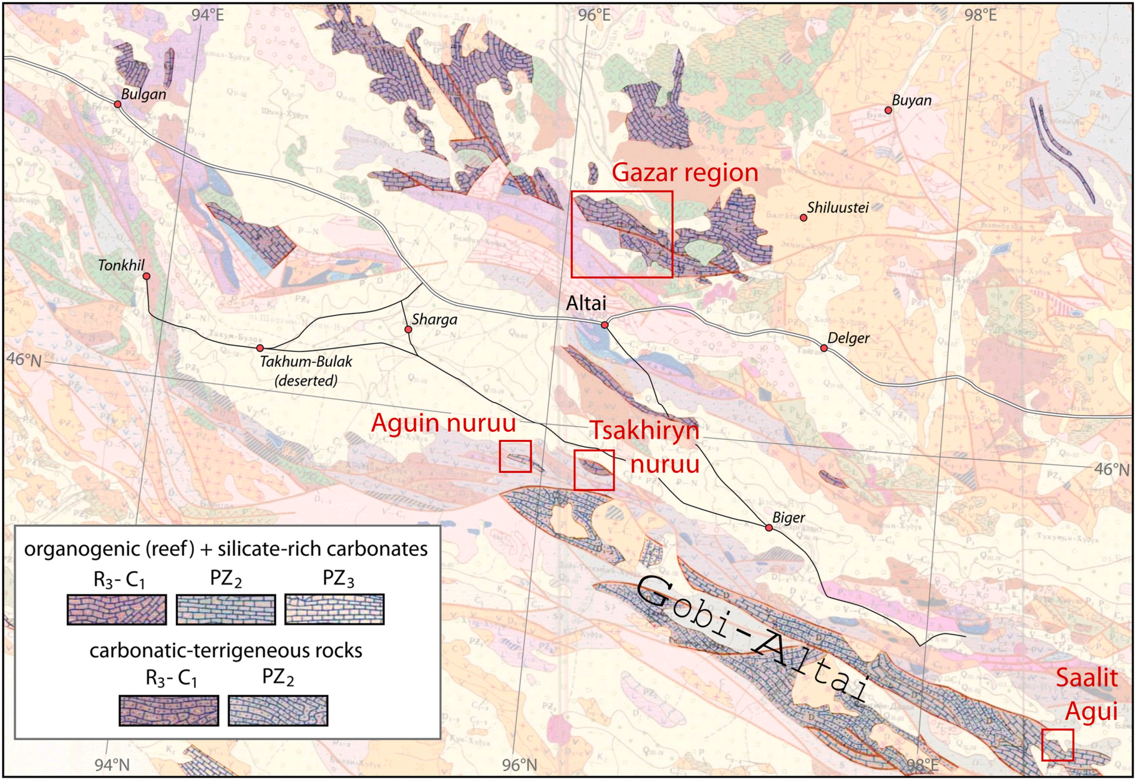

94°E
96°E
98°E
Bulgan
Buyan
Gazar region
Shiluustei
Tonkhil
Altai
Sharga
Delger
Takhum-Bulak
(deserted)
46°N
Aguin nuruu
Tsakhiryn
nuruu
46°N
Biger
Gobi-Altai
Saalit
Agui
94°N
96°N
98°E
organogenic (reef) + silicate-rich carbonates
R_3- C_1
PZ_2
PZ_3
carbonatic-terrigeneous rocks
R_3- C_1
PZ_2

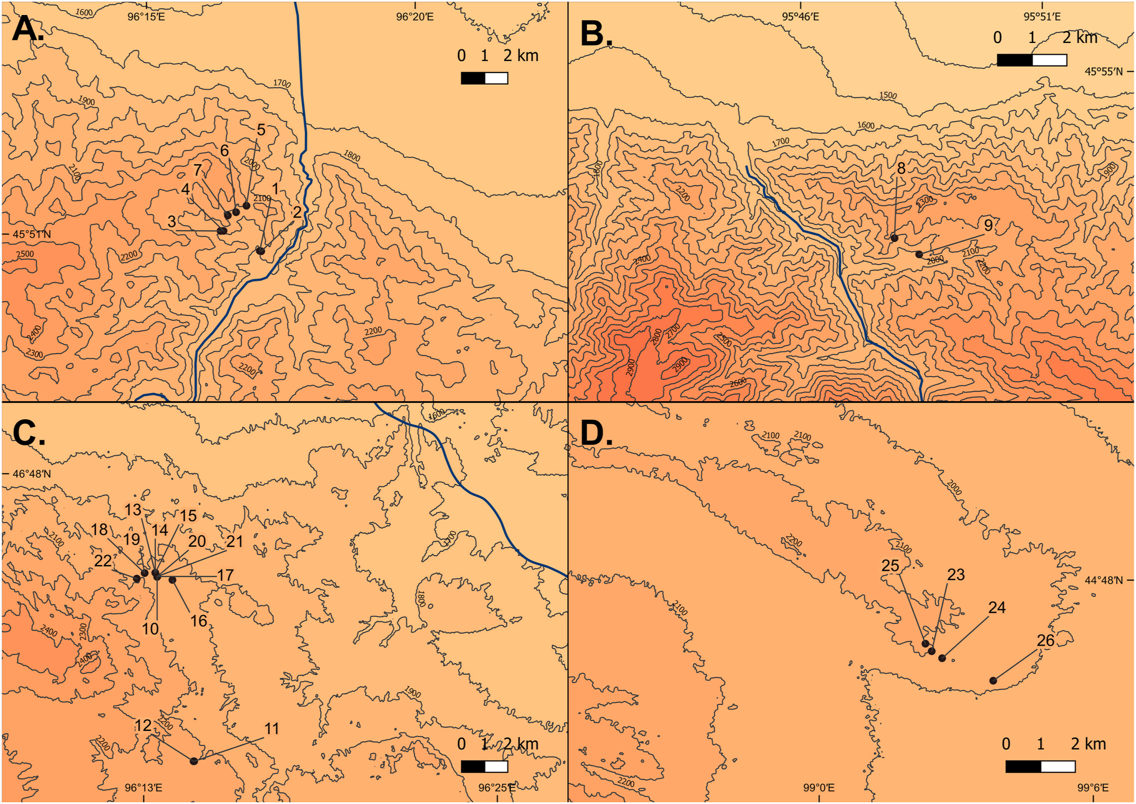

A.
96°15′E
96°20′E
0 1 2 km
45°51′N
1600
1700
1800
1900
2000
2100
2200
2300
2400
2500
1
2
3
4
5
6
7
B.
95°46′E
95°51′E
0 1 2 km
45°55′N
1500
1600
1700
1800
1900
2000
2100
2200
2300
2400
2500
2600
2700
2800
2900
8
9
C.
46°48′N
96°13′E
96°25′E
0 1 2 km
1600
1700
1800
1900
2100
2200
2300
2400
10
11
12
13
14
15
16
17
18
19
20
21
22
D.
44°48′N
99°0′E
99°6′E
0 1 2 km
2000
2100
2200
23
24
25
26

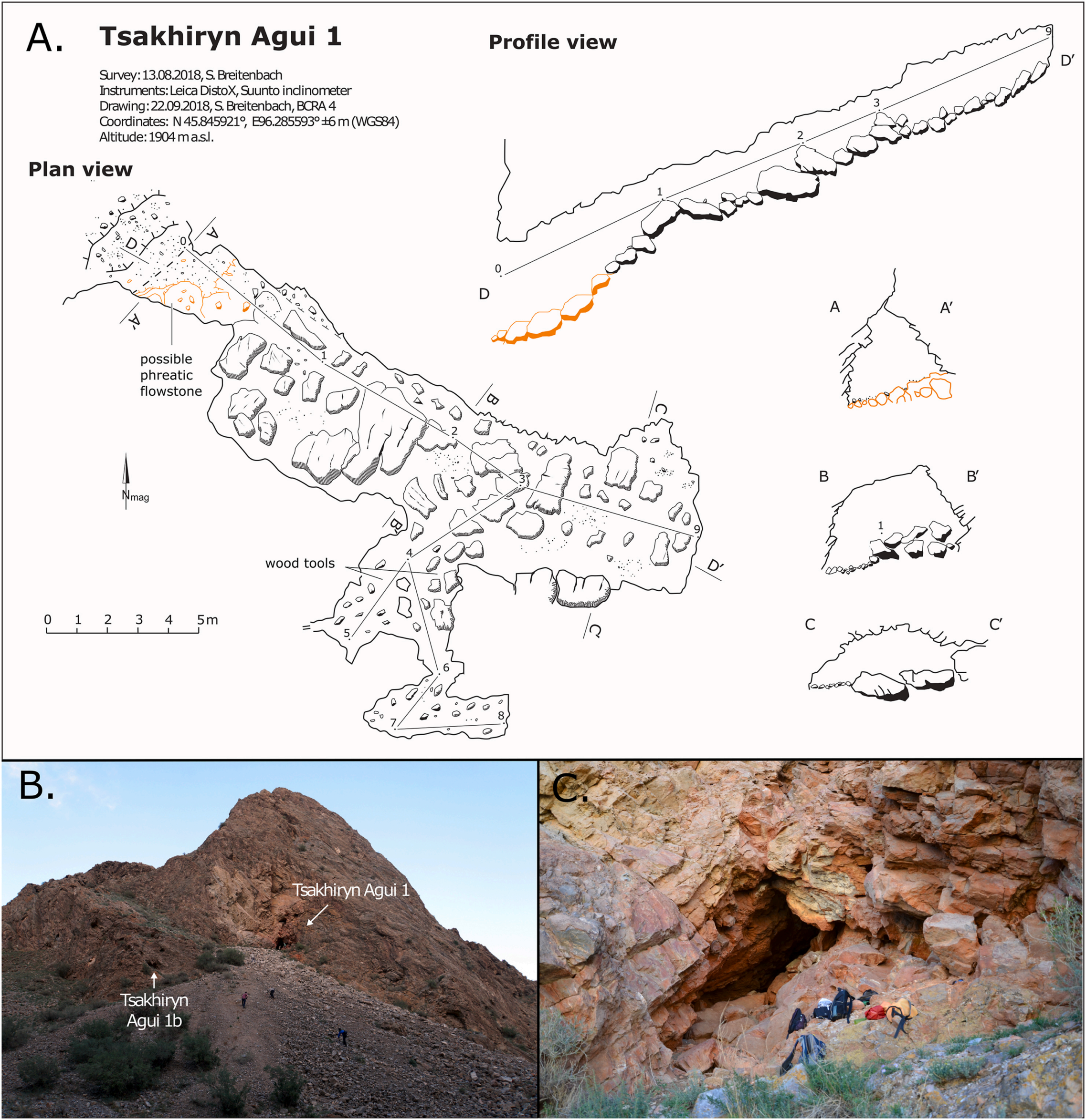
A.
Tsakhiryn Agui 1
Survey: 13.08.2018, S. Breitenbach
Instruments: Leica DistoX, Suunto inclinometer
Drawing: 22.09.2018, S. Breitenbach, BCRA 4
Coordinates: N 45.845921°, E96.285593° ±6 m (WGS84)
Altitude: 1904 m a.s.l.
Plan view
Profile view
possible phreatic flowstone
wood tools
Nmag
0 1 2 3 4 5 m
A A′
B B′
C C′
D D′
B.
Tsakhiryn Agui 1
Tsakhiryn Agui 1b
C.

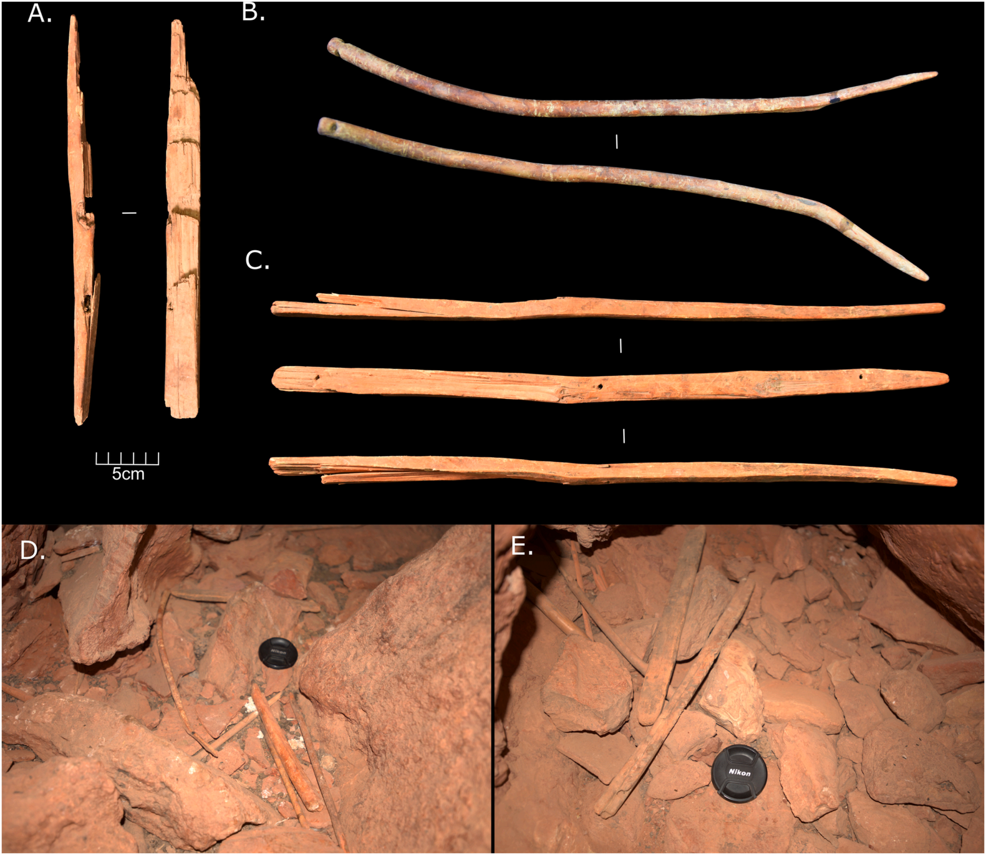
A.
B.
C.
D.
E.
5cm
Nikon
Nikon

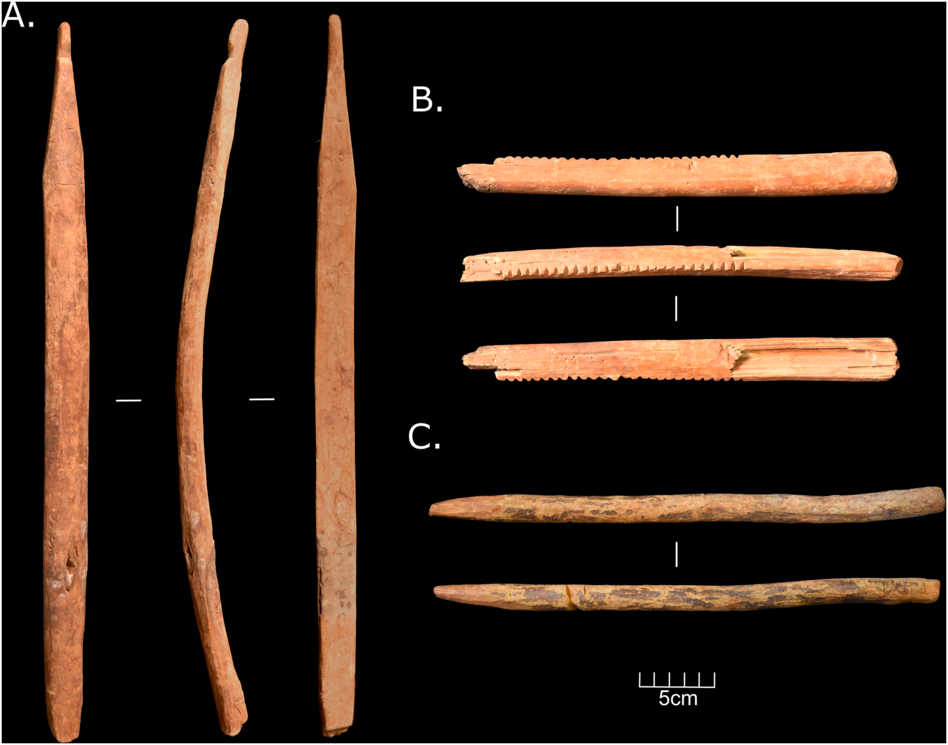
A.
B.
C.
5cm

Tsakhiryn Agui 4

Survey: 12.08.2018, S. Breitenbach & D. Sokolnikov
Instruments: Leica DistoX, Suunto inclinometer
Drawing: 22.09.2018, S. Breitenbach, BCRA 4
Coordinates: N 45°51'17.859", E96°16'54.587" ±10 m (WGS84)
Altitude: 2054 m a.s.l.

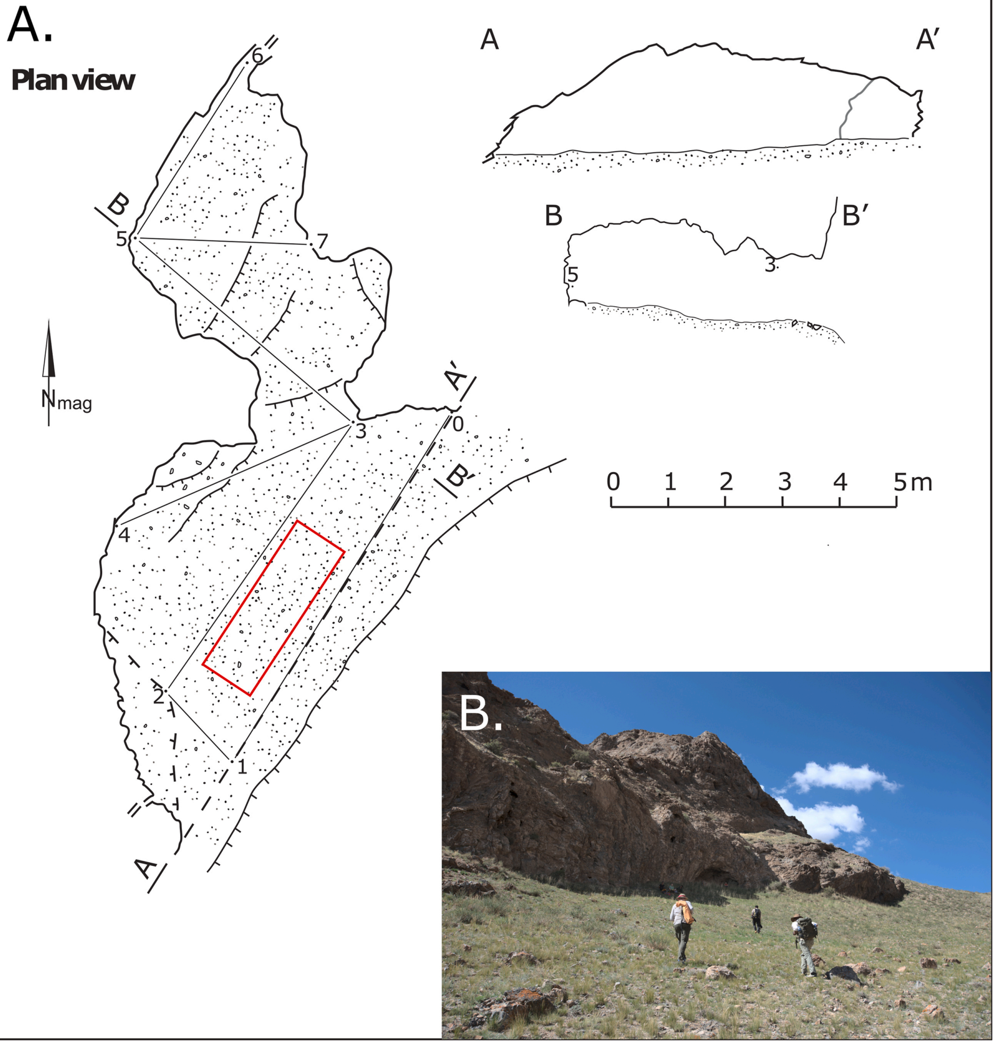

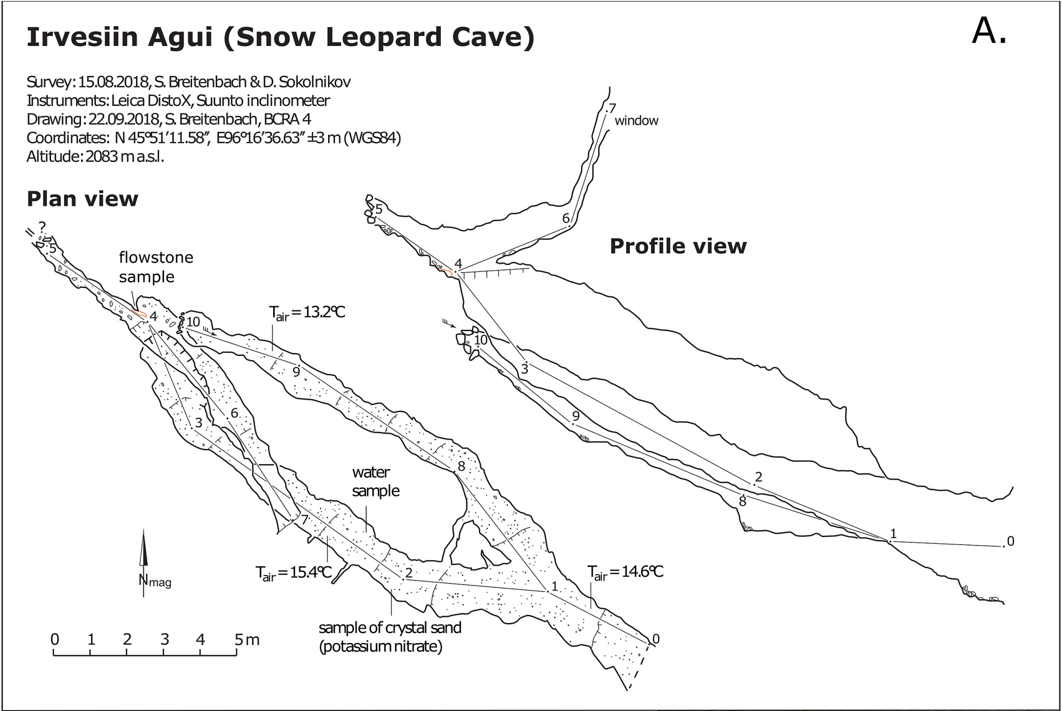
Irvesiin Agui (Snow Leopard Cave)
A.
Survey: 15.08.2018, S. Breitenbach & D. Sokolnikov
Instruments: Leica DistoX, Suunto inclinometer
Drawing: 22.09.2018, S. Breitenbach, BCRA 4
Coordinates: N 45°51'11.58", E96°16'36.63" ±3 m (WGS84)
Altitude: 2083 m a.s.l.
Plan view
Profile view
flowstone sample
window
water sample
sample of crystal sand (potassium nitrate)
T air = 13.2°C
T air = 15.4°C
T air = 14.6°C
N mag
0 1 2 3 4 5 m
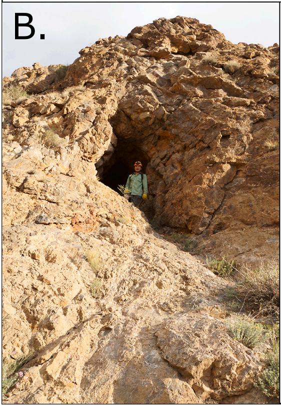
B.
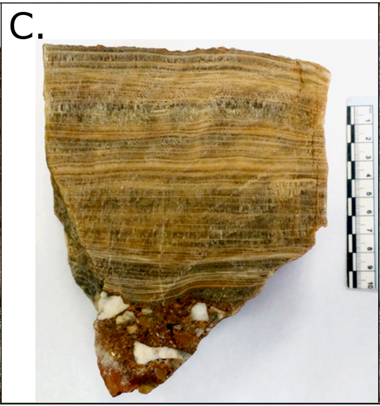
C.

D.

Nuramt Tsakhir Agui

Survey: 13.08.2018, S. Breitenbach
Instruments: Leica DistoX, Suunto inclinometer
Drawing: 22.09.2018, S. Breitenbach, BCRA 4
Coordinates: N 45.878726°, E95.793977° ±5 m (WGS84)
Altitude: 2092.2 m a.s.l.

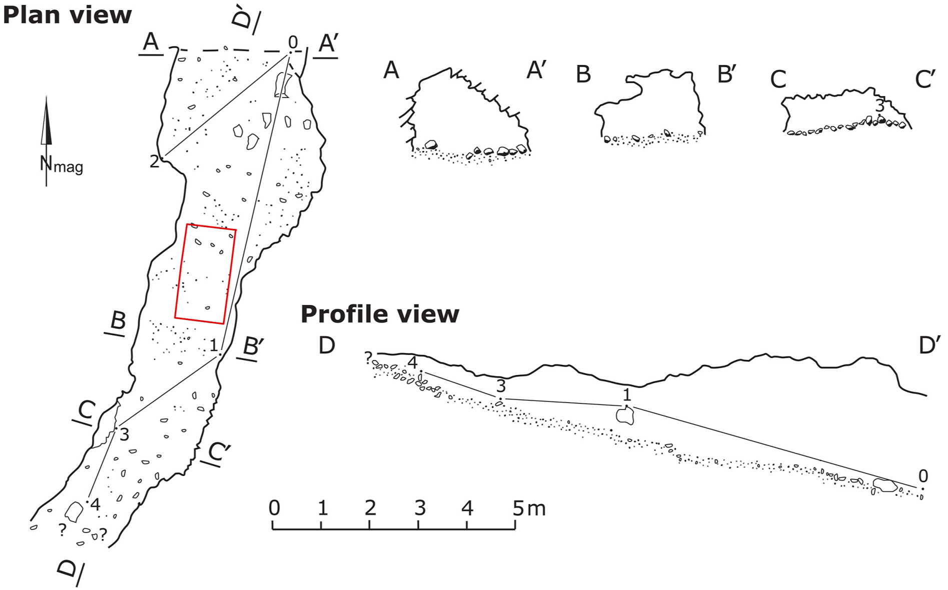

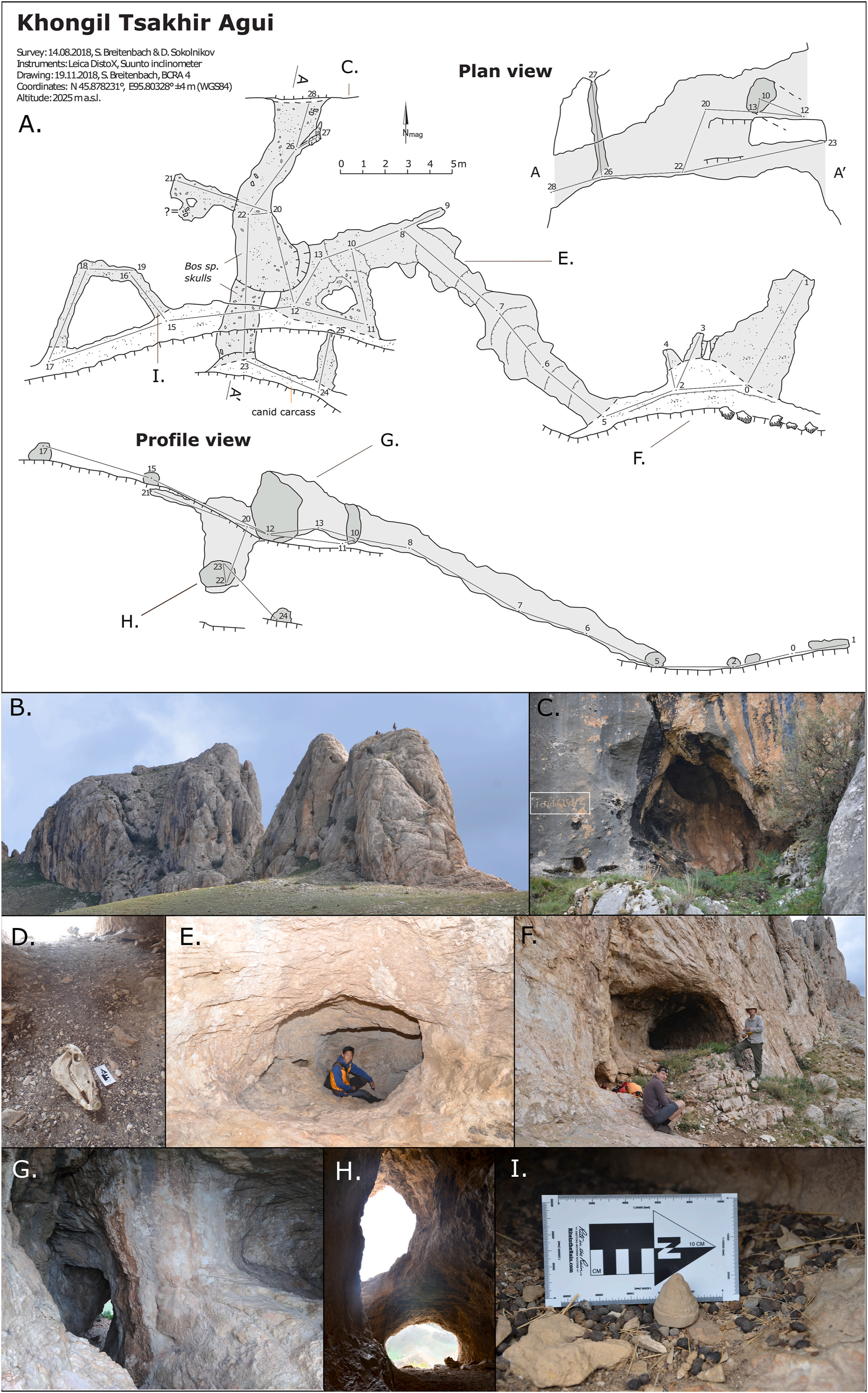
Khongil Tsakhir Agui
Survey: 14.08.2018, S. Breitenbach & D. Sokolnikov
Instruments: Leica DistoX, Suunto inclinometer
Drawing: 19.11.2018, S. Breitenbach, BCRA 4
Coordinates: N 45.878231°, E95.80328° ±4 m (WGS84)
Altitude: 2025 m a.s.l.
A.
Plan view
Profile view
N mag
0 1 2 3 4 5 m
Bos sp. skulls
canid carcass
A
A'
B.
C.
D.
E.
F.
G.
H.
I.

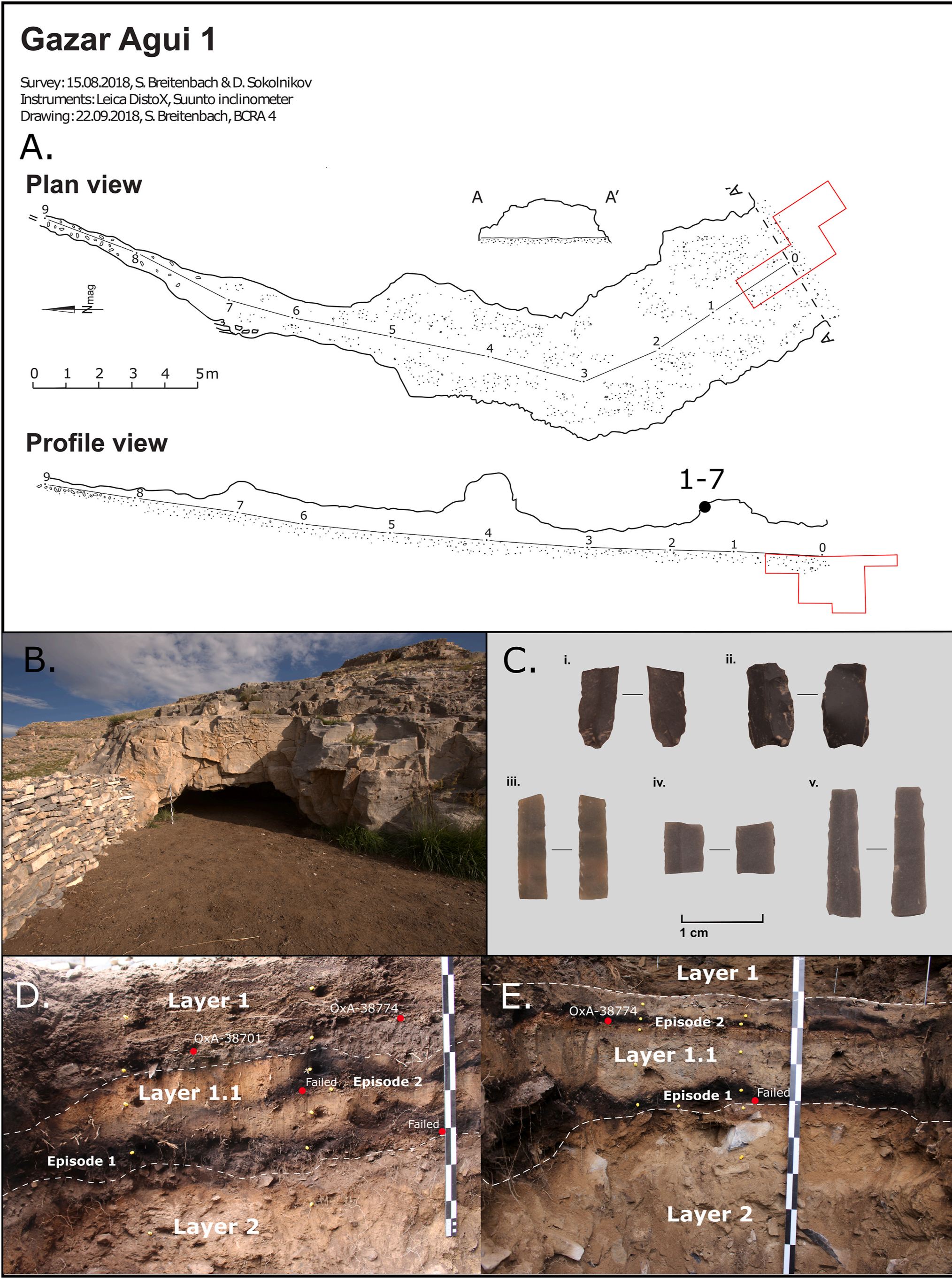
Gazar Agui 1
Survey: 15.08.2018, S. Breitenbach & D. Sokolnikov
Instruments: Leica DistoX, Suunto inclinometer
Drawing: 22.09.2018, S. Breitenbach, BCRA 4
A.
Plan view
A
A′
Nmag
0 1 2 3 4 5m
Profile view
1-7
B.
C.
i.
ii.
iii.
iv.
v.
1 cm
D.
Layer 1
OxA-38774
OxA-38701
Layer 1.1
Failed
Episode 2
Failed
Episode 1
Layer 2
E.
Layer 1
OxA-38774
Episode 2
Layer 1.1
Episode 1
Failed
Layer 2

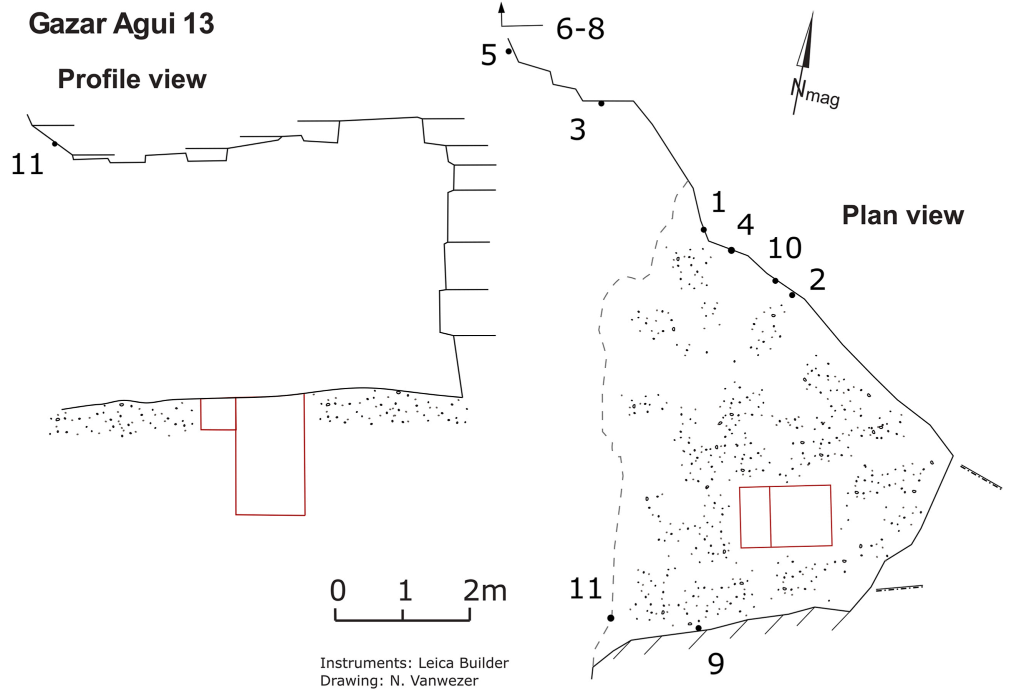

Instruments: Leica Builder
Drawing: N. Vanwezer

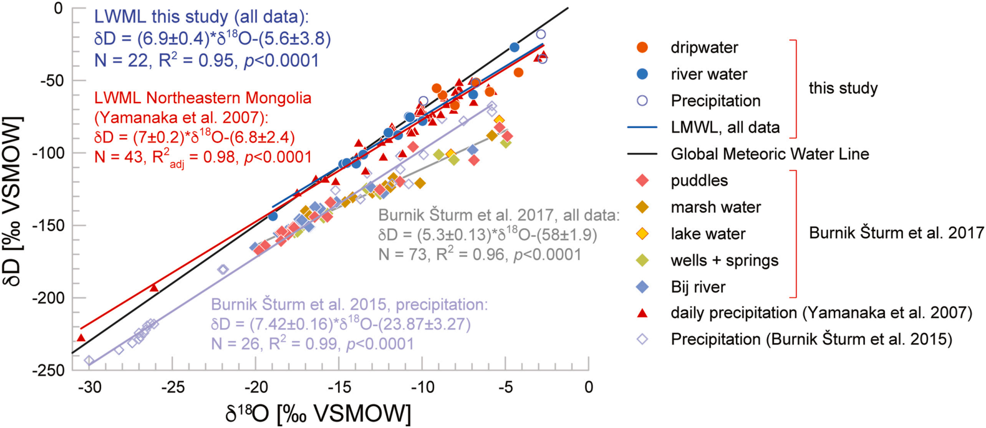

LWML this study (all data):
δD = (6.9±0.4)*δ18O-(5.6±3.8)
N = 22, R2 = 0.95, p<0.0001
LWML Northeastern Mongolia
(Yamanaka et al. 2007):
δD = (7±0.2)*δ18O-(6.8±2.4)
N = 43, R2adj = 0.98, p<0.0001
Burnik Šturm et al. 2017, all data:
δD = (5.3±0.13)*δ18O-(58±1.9)
N = 73, R2 = 0.96, p<0.0001
Burnik Šturm et al. 2015, precipitation:
δD = (7.42±0.16)*δ18O-(23.87±3.27)
N = 26, R2 = 0.99, p<0.0001
δD [‰ VSMOW]
δ18O [‰ VSMOW]
0
-50
-100
-150
-200
-250
-30
-25
-20
-15
-10
-5
0
dripwater
river water
Precipitation
LMWL, all data
this study
Global Meteoric Water Line
puddles
marsh water
lake water
wells + springs
Bij river
Burnik Šturm et al. 2017
daily precipitation (Yamanaka et al. 2007)
Precipitation (Burnik Šturm et al. 2015)

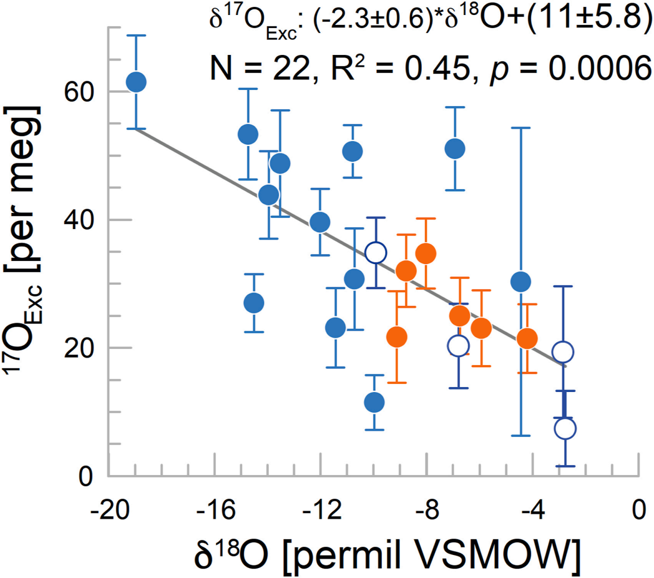

δ17OExc: (-2.3±0.6)*δ18O+(11±5.8)
N = 22, R2 = 0.45, p = 0.0006
60
40
20
0
17OExc [per meg]
-20
-16
-12
-8
-4
0
δ18O [permil VSMOW]

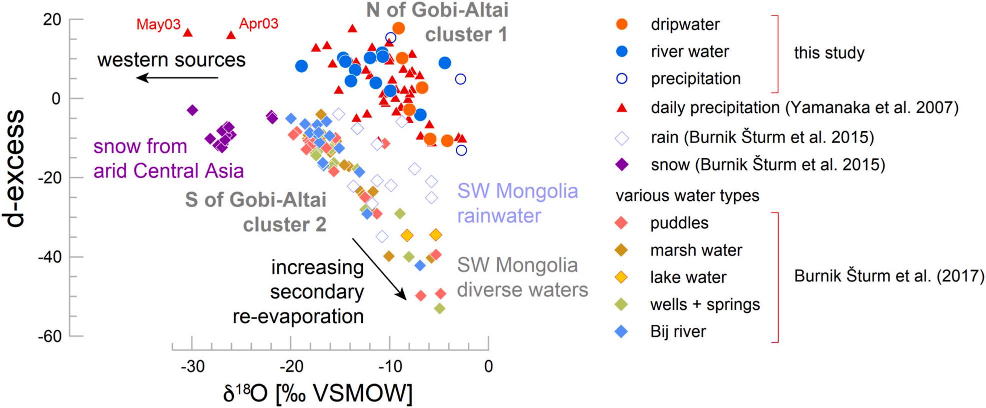

N of Gobi-Altai
cluster 1
May03
Apr03
western sources
snow from
arid Central Asia
S of Gobi-Altai
cluster 2
SW Mongolia
rainwater
SW Mongolia
diverse waters
increasing
secondary
re-evaporation
d-excess
δ18O [‰ VSMOW]
20
0
-20
-40
-60
-30
-20
-10
0
dripwater
river water
precipitation
this study
daily precipitation (Yamanaka et al. 2007)
rain (Burnik Šturm et al. 2015)
snow (Burnik Šturm et al. 2015)
various water types
puddles
marsh water
lake water
wells + springs
Bij river
Burnik Šturm et al. (2017)

Declaration of interests

☒ The authors declare that they have no known competing financial interests or personal relationships that could have appeared to influence the work reported in this paper.

☐The authors declare the following financial interests/personal relationships which may be considered as potential competing interests: